Synthetic Homes: A Multimodal Generative AI Pipeline for Residential Building Data Generation under Data Scarcity

Jackson Eshbaugh[1] Chetan Tiwari[2] Jorge Silveyra[1]

[1] Department of Computer Science
Lafayette College
Easton, PA, USA
[2] Department of Computer Science
Georgia State University
Atlanta, GA, USA

eshbaugj@lafayette.edu · ctiwari@gsu.edu · silveyrj@lafayette.edu

Preprint · Version 6.0 · July 2026

arXiv:2509.09794v6 [cs.AI] 10 Jul 2026

Abstract

Computational models have emerged as powerful tools for multi-scale energy modeling research at the building and urban scale, supporting data-driven analysis across building and urban energy systems. However, these models require large amounts of building parameter data that is often inaccessible, expensive to collect, or subject to privacy constraints. We introduce a modular framework that applies generative Artificial Intelligence (AI) to construct simulation-ready building datasets from publicly available records and imagery. To improve the reliability of this framework, we evaluate both its AI components and its overall result. Our occlusion analysis demonstrates that for our selected images, LLaVA achieves greater visual focus than a GPT-based alternative for building image processing. We also assess plausibility of our results against a national reference dataset, finding that our synthetic data overlaps more than 95% for three of the four selected variables. This work aims to reduce dependence on costly or restricted data sources, lowering barriers to building-scale energy research and Machine Learning (ML)-driven urban energy modeling, thereby providing simulation-ready datasets intended to support downstream applications such as energy modeling, retrofit analysis, and urban-scale simulation under data scarcity.

Keywords: Applied AI, Building Energy Modeling, Synthetic Data, Generative AI

1 Introduction

Consumption of electricity in the United States will increase by 1.7% between 2020 and 2026 (U.S. Energy Information Administration 2025) and seasonal electricity use per person has nearly doubled from 1973 to 2025 (U.S. Environmental Protection Agency 2025). Rising energy consumption exerts increasing pressure on infrastructure capacity, operational costs, and greenhouse gas emissions, resulting in rising costs for governments, energy producers, and energy consumers. Accurate modeling and policy tools are therefore essential for effective planning, helping prevent infrastructure strain, optimize energy costs, minimize or mitigate climate impacts, assess policy effectiveness, and guide decision-making in urban centers (Bompard et al. 2024; Perera et al. 2021; Zeng et al. 2011; Hajri et al. 2025).

Computational approaches to monitor energy usage and model urban centers, buildings, and other structures require large amounts of data, such as type and quality of materials, floor plans, and weather patterns to produce scalable and quantitative results (U.S. Department of Energy 2025). However, several

issues arise when attempting to collect such information, including high prices, limited availability, and privacy concerns. These issues create barriers to accessing data, hindering the development of accurate models and the scaling of models to larger populations or geographic areas. The inaccessibility of this data has led researchers to generate synthetic data through a variety of methods.
The primary contributions of this work are:

- A modular framework that applies multimodal generative AI to residential building energy modeling by integrating publicly available records, imagery, and physics-based simulation into a unified workflow for producing simulation-ready residential datasets;
- An end-to-end implementation demonstrating that the framework generates 247 synthetic simulation-ready homes at a worst-case cost of $0.0039 per home while reducing the expertise and data-access barriers associated with residential energy modeling;
- An occlusion-based analysis approach that provides insight into visual feature usage in language models for building understanding; and
- A quantitative evaluation demonstrating that the generated data is plausible when evaluated against ResStock (Present et al. 2024).

In the following sections, we position our work in the existing literature (Section 2) and provide an in depth view of our framework (Section 3). Then, we evaluate the plausibility of data generated by our pipeline (Section 4) and we conclude and highlight future directions from this work (Section 5).

2 Related Work

Current data generation efforts span a wide range of approaches, from optimizing building construction processes to the creation of digital twins. For example, Wan et al. (2022) built a generative model that improves the efficiency of energy consumption by determining the optimal layout of floor plans. Elnabawi and Hamza (2022) enhanced their building energy models using highly detailed microclimate models that considered features such as shadow generation and seasons to generate weather data. Lee et al. (2019) train a neural network that predicts building energy consumption, aiming to create a more robust model with limited real-world measurements. The network was trained with data synthesized using, among others, electricity, temperature, and humidity, encoded into receiver operating characteristic (ROC) plots which visually encode the separation between classes and are commonly used to assess model discrimination (Zweig and Campbell 1993; Janssens and Martens 2020).

Other researchers focus on creating and applying digital twins: virtual, dynamic, and data-driven digital replicas of real-world urban environments. Stinner et al. (2021) generate digital twins of building energy systems from piping and instrumentation diagrams using convolutional networks and other algorithms. Agostinelli et al. (2021) create digital twins of energy efficient buildings in residential areas from Building Information Modeling (BIM), Internet of Things (IoT), Geographical Information Systems (GIS), and AI components, with machine learning serving as the central module of the model. Francisco et al. (2020) take a different approach by generating digital twins of daily, time-segmented energy benchmarks solely from smart meter data streams. Belik and Rubanenko (2023) present a hybrid digital twin framework for renewable energy sources (RES) that integrates real-time data, 3D modeling, and sensitivity analysis to improve forecasting and operational efficiency, particularly in grid systems with high RES penetration.

While prior work has focused on traditional simulation tools or sensor data to construct digital twins, H. Xu et al. (2024) encourage the use of generative AI models, such members of the GPT family, because they present new opportunities in urban data generation. For instance, Dodge et al. (2017) employ convolutional neural networks (CNNs) to parse floor plan images, generating structured representations using wall

segmentation, object recognition, and optical character recognition. Relatedly, L. Zhang et al. (2025) implement a pipeline that generates EnergyPlus IDF files from initial building geometry and textual building descriptions. Moreover, Xiao and P. Xu (2024) propose a multi-agent Large Language Model (LLM) framework that processes unstructured building data and sensor logs to support automated energy optimization in smart grid contexts. Additionally, in closely related fields, generative AI has been successfully employed to perform a variety of tasks, such as predictive analysis of traffic congestion (Lin et al. 2025), real-time decision-making in urban air mobility (Sha et al. 2024), and stochastic solar irradiance forecasting for building facades (Y. Zhang et al. 2022).

M. Liu et al. (2025) present a wide-ranging review on the integration of generative AI into building energy workflows, highlighting both opportunities and challenges. These include concerns such as dataset preparation, hallucinations, and a lack of domain-specific expertise. However, the impact of such challenges varies depending on the pipeline design. Because our framework combines pretrained LLMs with simulation tools for quantitative evaluation, we avoid the need for fine-tuning or physics-aware generation, thereby reducing the impact of these concerns. Moreover, we evaluate our framework's LLM components to avoid generating data impacted by hallucinations. Additionally, Liu emphasizes the importance of multimodal integration—where multiple data modalities (such as image, text, and tabular data) are used by a process or model. Producing high-quality structured urban data suitable for tasks such as modeling and simulation requires combining multiple complementary processes into a single workflow (Rehmann et al. 2025; Guo et al. 2023; Bishop et al. 2024). We adopt these principles in the design of our general framework.

While prior work has explored using individual and joint components of synthetic building data generation, our contribution is a modular framework that composes a unified workflow for generating synthetic simulation-ready residential energy datasets from publicly available information. By combining assessor records, street-level imagery, multimodal foundation models (LLaVA and GPT), and EnergyPlus-compatible output generation, the framework could substantially reduce the expertise, data acquisition, and financial barriers traditionally associated with residential energy modeling.

The framework also produces multimodal outputs, including both structured building characteristics suitable for simulation and natural-language inspection notes that can be used for future machine learning and decision-support tasks. Collectively, these capabilities make it possible to generate complex residential energy datasets through a largely automated workflow, enabling broader participation in building energy research in settings where detailed building inventories are unavailable or prohibitively expensive to obtain.

3 Methodology

We introduce a reusable framework for generating simulation-ready residential datasets from publicly available information under conditions of data scarcity. The framework combines heterogeneous public records, generative AI models, and physics-based simulation into four modular components, depicted in Figure 1. Each stage focuses on a transformation of the data, from data collection to simulation:

1. A web scraper that collects data and images;
2. An image processor powered by LLaVA (H. Liu, C. Li, Wu, et al. 2023);
3. A Geographic JSON (GeoJSON) and inspection note generator using GPT (OpenAI 2025); and
4. An EnergyPlus[1] (Crawley et al. 2001) simulation

While our pipeline is tailored to generate data from images and tabular data, it is inherently modular and extensible. Any stage is easily modified or expanded for other related purposes, and different information can be generated in addition to or in place of any data produced by this pipeline. For example, a different

[1]EnergyPlus™ is a trademark of the United States Department of Energy.

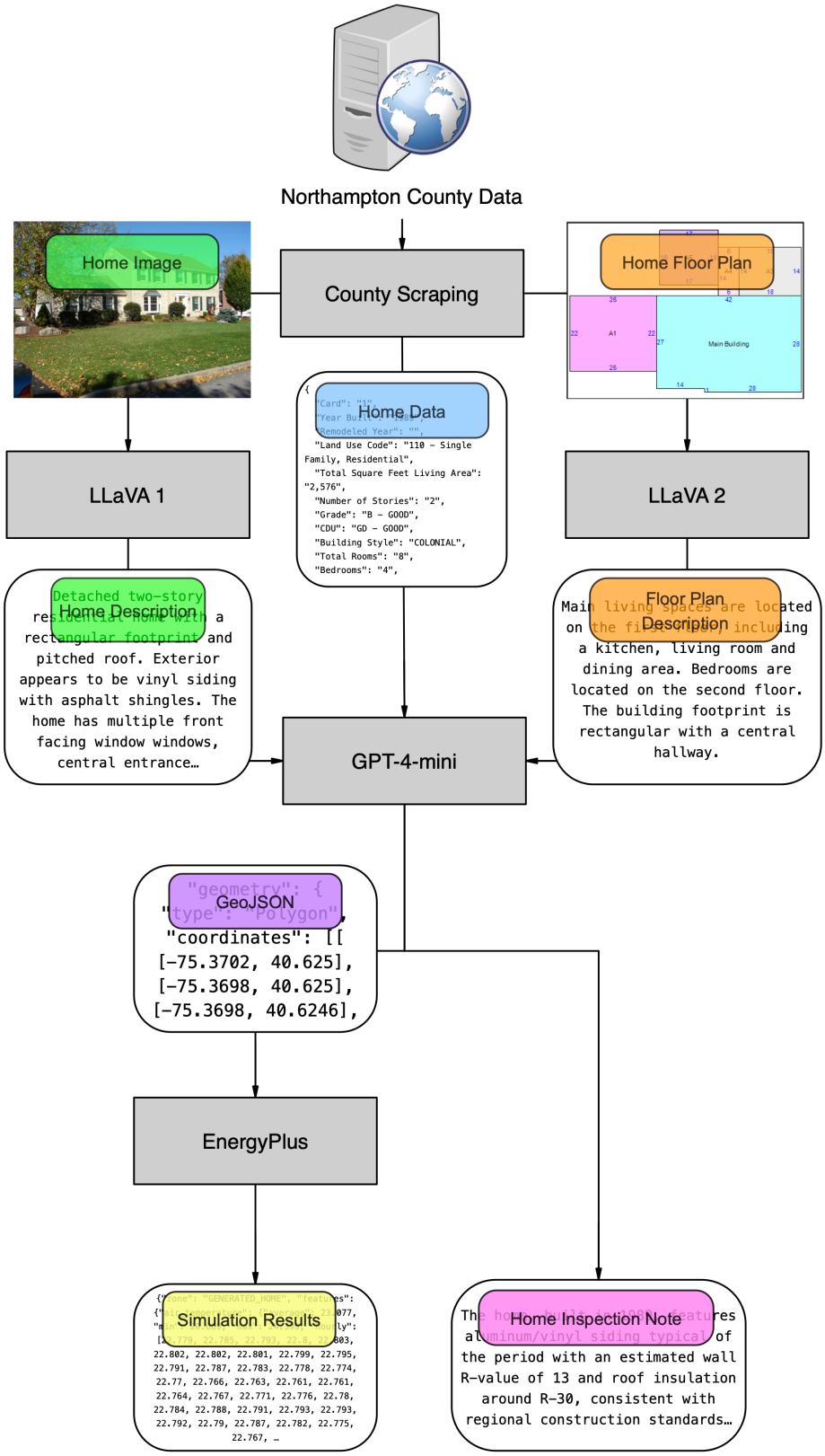


Figure 1. Overview of the pipeline.

LLM could be employed in place of GPT, or other types of data could be considered or generated by the pipeline. Those interested in generating synthetic commercial buildings could use a modified version of this pipeline that emphasizes the characteristics and data central to their research. This opens use of our work to a larger set of individuals. Rather than proposing a rigid set of steps, we present a flexible framework that integrates generative AI, web scraping, and building simulation, designed for rapid, low-cost data generation in building energy and other fields that traditionally suffer from data scarcity. Ultimately, the data generated by our framework can be used to prototype, design, train, and research urban energy systems and models.

An instance of this pipeline was implemented and executed[2] on a `g3.medium` flavor JetStream 2 virtual machine running Ubuntu 24.04.2 (Noble). Specifically, the system featured one NUMA node with 8 AMD EPYC-Milan processors, 30 GB of RAM, and an NVIDIA A100 SXM4 40 GB GPU (of which 10 GB was allocated). Additionally, it was fully virtualized (KVM and AMD-V). We paid $0.73 (USD) for OpenAI requests to produce data for 247 homes—about $0.0030 per home.[3] To run the pipeline, we used the PyTorch (Ansel et al. 2024) machine learning framework, and the Hugging Face Transformers library (Wolf et al. 2020) to load the models we used. In the subsections that follow, we describe each pipeline component in detail.

3.1 Scraping the Data

To ensure the synthetic data we generated reflects real-world homes, we collected data from publicly available county datasets. For our pipeline instance, we gathered data from Northampton County, Pennsylvania, where two of the authors work and reside. To collect this data, we implemented a web scraper using `Selenium WebDriver` (Selenium 2024) and `ChromeDriver` (Google 2023). For each residential property on each street in the list of streets to process, the scraper extracts key attributes, such as number of rooms, total floor area, and other metadata listed in Table 1. This data is saved to a JavaScript Object Notation (JSON) file for each home. Additionally, the scraper downloads two images: a street view photograph and a floor plan, both of which are made available on the County's public-facing platform. An example of each is depicted in Figure 2.

Although this implementation targets a single county, the pipeline is modular and can be adapted to different public record schemas and regional metadata formats. Currently, our scraper is configured to gather information from Northampton County's instance of iasWorld. Developed by Tyler Technologies, iasWorld is an Enterprise Assessment & Tax solution used by "jurisdictions in 26 US states, four Canadian provinces, and the Bahamas" (Tyler Technologies 2022). However, our implementation could easily be modified to point to another instance, such as in DeKalb County, Georgia.

Moreover, multiple web scraping modules could be employed to gather data from differently structured systems simultaneously. For example, Lancaster County, Pennsylvania uses a tool by Devnet called Edge. To create a dataset consisting of homes in Lancaster, Northampton, and DeKalb county, simply create two versions of the scrapers, one for Devnet and one for iasWorld. While much of the high-level scraping logic would remain consistent across systems, the underlying HTML structure, identifiers, and parsing rules would require tool-specific adjustments. Nevertheless, the modular design of the ingestion pipeline allows these adaptations to be incorporated without changing the overall framework.

[2]Source code: https://github.com/Lafayette-EshbaughSilveyra-Group/synthetic-homes.

[3]Assuming a conservative upper bound of 10 CPU minutes per home at 100 watts and electricity prices at $0.15 per kilowatt-hour, local electricity costs are approximately $0.0025 per synthetic home, giving a worst case total of $0.0055 per synthetic home.

Collected Data	**Type**
Year Built	Year
Remodeled Year	Year
Land Use Code	String
Total Square Feet Living Area	Number
Number of Stories	Number
Grade	String
CDU	String
Building Style	String
Total Rooms	Number
Bedrooms	Number
Full Baths	Number
Half Baths	Number
Additional Fixtures	Number
Total Fixtures	Number
Heat/Air Cond	String
Heating Fuel Type	String
Heating System Type	String
Attic Code	String
Unfinished Area	Number
Rec Room Area	Number
Finished Basement Area	Number
Fireplace Openings	Number
Fireplace Stacks	Number
Prefab Fireplaces	Number
Basement Garage (Number of Cars)	Number
Condo Level	Number
Condo/Townhouse Type	String
Basement	String
Exterior Wall Material	String
Physical Condition	String
Sketch Data	Dictionary of floorplan segment areas

Table 1. All data we collected from the county portal. Not all homes have values for each variable.

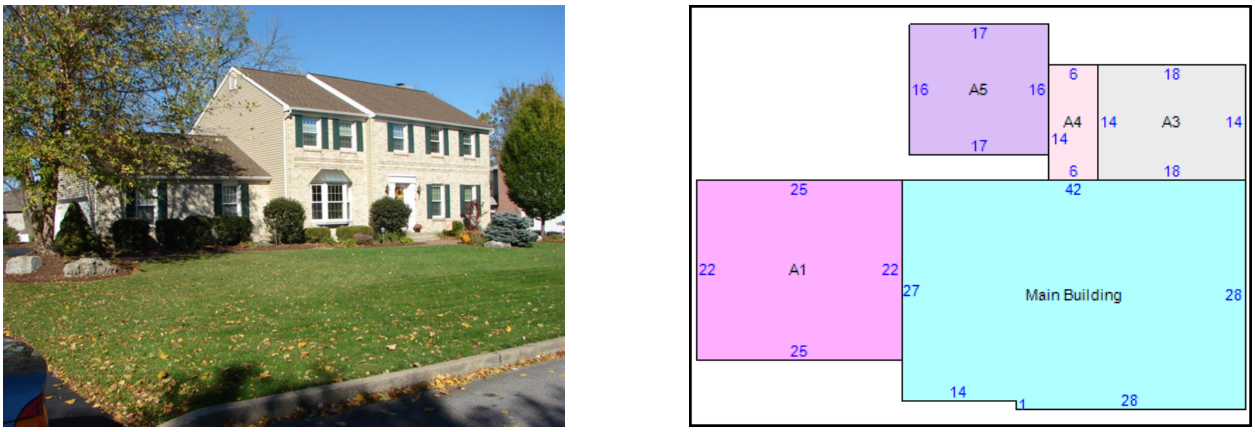


Figure 2. An example street view photograph and floor plan from the Northampton County database.

3.2 Processing Images

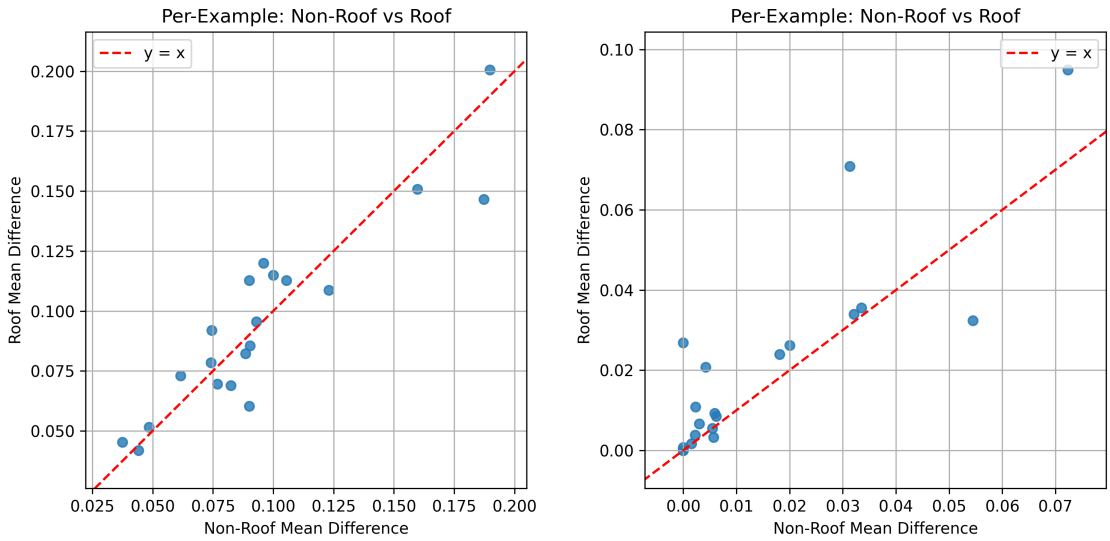
After scraping the street view photographs and floor plans from the county portal, they are analyzed using LLaVA (H. Liu, C. Li, Wu, et al. 2023) version 1.5 with 7 billion parameters, distributed on HuggingFace (`llava-hf/llava-1.5-7b-hf`). This step processes both files to translate them into a textual description. For example, the floor plans can be used to define the geometry of the home, and the image to determine the quality and number of windows. The goal of utilizing the floor plan image is not to generate a one-to-one replication of a given home, but instead, it is used to produce structurally plausible layouts. This allows our pipeline to infer important aspects of the homes that will be used to generate the GeoJSON, which is ultimately used to generate the Input Definition File (IDF) file required by EnergyPlus.

3.2.1 Evaluating Visual Focus with Occlusion Testing

In image processing, it is crucial that only key portions of the images in question trigger differences in the response of a model. For example, if the prompt asks about the state of the roof of a home, the tree next to the home should be inconsequential in comparison to the roof itself. In this document, we refer to this measure as *focus*. Following, we present an evaluation of focus using occlusion, which is intended to measure differential sensitivity rather than measuring semantic correctness or providing a formal visual attribution method.

Occlusion measures the necessity of a part of an image: if removing a feature causes the prediction to change, that feature was necessary for the model's decision (Hooker et al. 2019; Balkir et al. 2022). When we remove image portions, we replace them with a neutral value, such as black. This creates a masked version of the image. The degree of change measured between the model's output for this masked image and its baseline response reflects the importance of the masked cell. High sensitivity to the removal of a feature suggests the model relied heavily on that region to produce its output, indicating that the region was internally necessary to the model's decision process.

During the development of our pipeline, we identified two candidate LLMs to employ for image processing. To determine the best model for this task, we compared the focus of the GPT and LLaVA LLMs when analyzing images using occlusion tests. We provided the models with twenty different images of homes: ten with roofs showing no signs of damage, and ten with roofs with significant damage. Each model was instructed to evaluate and describe the state of the roof and justify its evaluation. We first took a baseline where no part of the image was masked. Then, the image was divided into one hundred cells, a number we selected to balance effectiveness, efficiency, and cost. Each cell of the image was masked, and the model was executed on the original prompt and this new image. Textual responses were embedded into vectors



(a) GPT results.

(b) LLaVA results.

Figure 3. GPT and LLaVA forward occlusion per image results.

using the `all-MiniLM-L6-v2` SentenceTransformers model (Reimers and Gurevych 2019), a lightweight and widely used model sufficient for obtaining sentence-level numerical representations. Then, to measure the semantic difference between each execution of the experiment, we took the cosine distance of each embedded response from the baseline. Additionally, heatmaps of these differences were assembled using `matplotlib` (The Matplotlib Development Team 2025).

We categorize cells as follows: if a cell contains any visible portion of the roof, it is a roof cell; otherwise, it is considered a non-roof cell. This categorization was performed manually for all twenty images. The mean difference value in roof cells and non-roof cells for each image was calculated. Figure 3 depicts the distribution of the forward occlusion results. These scatter plots are particularly telling—GPT (Figure 3a) evenly scatters the data points on either side of the line $y = x$, indicating it has no preference for which area in the image is considered important. In comparison, LLaVA (Figure 3b) tends to produce results in the upper half of the graph. These results illustrate that, unlike GPT, LLaVA consistently exhibits greater sensitivity to roof regions than to non-roof regions, indicating stronger task-relevant visual focus in our occlusion experiments.

Additionally, overall means and standard deviations were calculated for GPT and LLaVA (Figure 4). In a well-focused model, the mean difference in the relevant area should be greater than the mean difference anywhere else. This behavior occurs since relevant cells should account for the majority of the response given by the model. In our experiments, we observe that GPT reports identical roof and non-roof mean differences (Figure 4a). However, LLaVA achieved a roof mean difference approximately 20% greater than its non-roof mean difference (Figure 4b).

Cells were partitioned into roof and non-roof groups within each image. The difference between the mean occlusion effects of the two groups was computed for each image and subsequently averaged across all images to obtain the mean paired difference (MPD). This value is a numerical representation of the relative importance of both cells that depict the roof and those that do not. Thus, the sign of the MPD indicates which cell group produced the larger occlusion effect, while its magnitude reflects the size of the difference. The results are reported in Table 2.

To assess whether the MPD is statistically significant, we employed paired Wilcoxon signed-rank tests

	Mean Difference	SD
Roof	0.0956	0.0384
Non-Roof	0.0956	0.0408

(a) GPT occlusion overall statistics

	Mean Difference	SD
Roof	0.0208	0.0241
Non-Roof	0.0149	0.0197

(b) LLaVA occlusion overall statistics

Figure 4. Occlusion statistics for GPT and LLaVA.

due to the small sample size and the non-normal, zero-heavy distribution of the differences. A statistically significant result ($p < 0.05$) indicates that the roof and non-roof mean differences are distinct for the given language model. GPT showed no statistically detectable difference between roof and non-roof regions ($p = 0.729$), while LLaVA demonstrated significantly greater roof-region sensitivity ($p = 0.0086$) with a moderate paired effect size ($d_z = 0.463$). Although occluding both roof and non-roof regions altered LLaVA's responses, the significantly larger occlusion effects observed for roof regions indicate that the model relied more heavily on task-relevant visual information. These statistical findings are summarized in Table 2.

Model	**Mean Paired Difference**	**Wilcoxon p-value**	**Cohen's d_z**
GPT	−0.000055	0.729	−0.003
LLaVA	0.005880	0.0086	0.463

Table 2. Paired roof-minus-non-roof occlusion differences by model. Mean paired difference is defined as roof mean difference - non-roof mean difference.

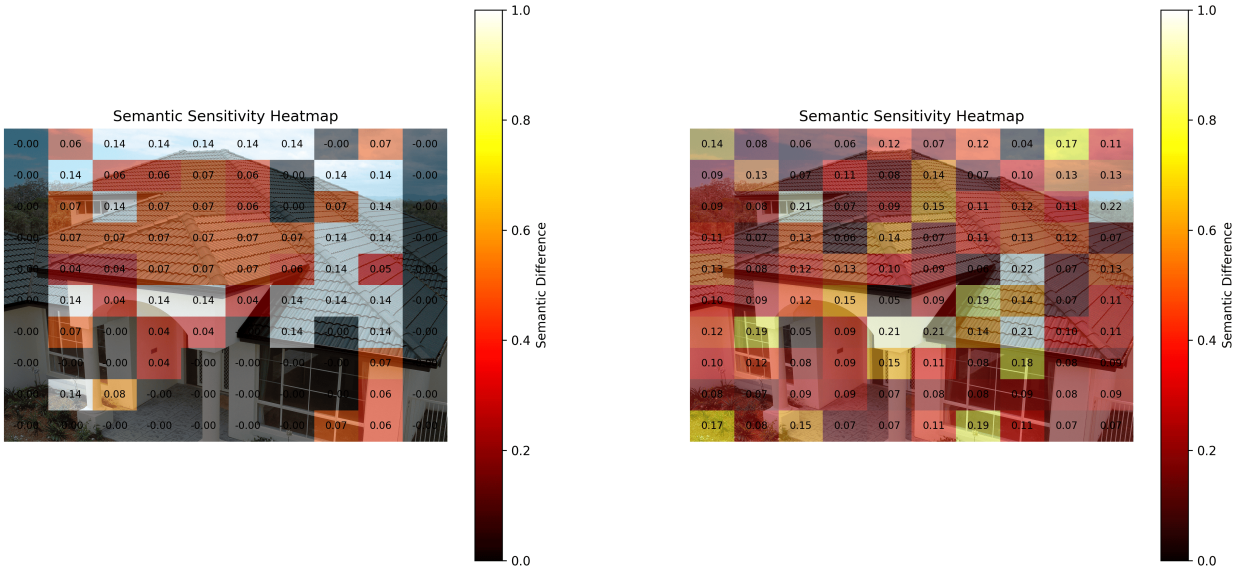
When we compared our individual GPT and LLaVA occlusion results, we found that LLaVA has greater roof-region sensitivity. LLaVA is much more particular about which cells are key to construct the response; GPT produces results that look stochastic. Figure 5 displays one noteworthy example—LLaVA focuses on a more specific section of the image, primarily consisting of the home's roof. GPT, on the other hand, behaves much more randomly. Each value in the cell is the semantic difference, and the background tint of the cell represents the scaled semantic difference, where the brightest background represents the largest difference and the darkest represents the smallest. In Figure 5a, the semantic difference is generally larger on the roof than on other parts of the image. A small semantic difference is a signal that a given portion of the image is less important to the model in order while formulating a response. In Figure 5b, the majority of cells are moderately important to the model in formulating a response—even cells containing walls or grass. Comparing the two, LLaVA demonstrates better focus on the more important parts of the image. Full occlusion experimental details, hypotheses, and findings are available in A.

The goal of the occlusion experiments was not to evaluate the quality of the image-to-text translation, as this aspect has been examined extensively in prior work by the model's developers (H. Liu, C. Li, Wu, et al. 2023; H. Liu, C. Li, Y. Li, et al. 2024). Those studies report strong performance on image description tasks, motivating our use of LLaVA as the image description component of the pipeline.

3.3 Generating GeoJSON

Once the images are processed, we utilize the descriptions given by LLaVA in a GPT prompt, available in B, to generate a GeoJSON file and home inspection notes. The prompt provides the image descriptions (Section 3.2) and data that was scraped from the county portal (Section 3.1) and directs the model to take two actions:

- The prompt instructs GPT to generate a GeoJSON file for the building, including geometry, data from the county, and five estimated performance parameters. These estimated parameters, defined according



(a) LLaVA occlusion results. These results show less sensitivity and more focus on roof cells compared to non-roof cells.

(b) GPT occlusion results. The model exhibits highly variable responses to image occlusions, indicating limited spatial selectivity between roof and non-roof regions.

Figure 5. GPT and LLaVA occlusion results.

to standard convention, include the HVAC heating and cooling coefficients of performance and R-values for the roof and wall.

- The prompt directs GPT to write a short inspection note, focused on energy-related observations such as insulation, HVAC type/age, visible windows, and any inferred upgrades. This inspection note is placed in the GeoJSON file.

The prompt contains strict guidelines intended to improve output validity, completeness, and simulation-oriented realism. In the pipeline, generated building footprints are additionally constrained using metadata-derived target footprint area estimates based on the reported living area and number of stories for each home. The prompt explicitly instructs GPT to generate compact residential-scale geometries whose footprint approximately matches the target estimate derived from the metadata. After generation, the area of the resulting geometry is validated against the reported footprint area. Given that most footprints are characteristically rectangular, we validate accuracy of the generated home by comparing the area of the generated footprint with the reported values.

If the area of the generated footprint falls outside the acceptable scale range, defined in our experiments as between 0.5× and 2.5× the true square footage of the home, the pipeline automatically reprompts GPT with corrective feedback regarding the size of the generated geometry. When more than six generation attempts fail to satisfy this constraint, a deterministic scaling correction is applied to improve footprint consistency while preserving the overall building shape. Table 3 shows the number of generation attempts required for each home. Of the 247 generated homes, 116 (47.0%) satisfied the geometric constraint on the initial generation. The remaining 131 homes required at least one regeneration, with progressively fewer requiring additional attempts. Only two homes (0.8%) exhausted all six generation attempts and required deterministic scaling.

To evaluate scale consistency between the synthetic homes and the original residential metadata, we compared generated footprint areas against county-derived target footprint estimates computed from the

Generation Attempts	Homes	Percent	Cumulative Homes
1 (accepted immediately)	117	47.4%	117
2	70	28.3%	187
3	35	14.2%	222
4	14	5.7%	236
5	6	2.4%	242
6	3	1.2%	245
Deterministic scaling	2	0.8%	247
Total	**247**	**100.0%**	**247**

Table 3. Number of generation attempts required before satisfying the area footprint constraint. Only two homes required deterministic scaling after exhausting all six generation attempts.

```geojson
{
  "type": "Feature",
  "properties": {
    "name": "Generated Home",
    "floor_area": 2576,
    "building_type": "Single family",
    "inspection_note": "...",
    "hvac_heating_cop": 0.85,
    "hvac_cooling_cop": 3.0,
    "wall_r_value": 13,
    "roof_r_value": 30,
  },
  "geometry": {
    "type": "Polygon",
    "coordinates": [...]
  }
}
```

Figure 6. Excerpt of a generated GeoJSON file.

reported living area and number of stories for each home. Generated footprint areas exhibited a statistically significant positive correlation with these metadata-derived target areas ($r = 0.3383$, $p < 0.001$; $R^2 = 0.1145$).

While the previous analysis evaluates the plausibility of the area of the generated homes, it does not address the reliability of the underlying structured-data generation process. We use GPT for structured data generation given its strong ability to produce well-formed JSON outputs from descriptive prompts. Prior work has demonstrated that LLMs can reliably generate outputs that conform to predefined schemas under strict schema constraints, even with no previous prompting or task-specific fine tuning. For example, the StructuredRAG benchmark suite showed 82% format compliance under JSON prompt conditions (Shorten et al. 2024).

As we built the pipeline, we reviewed GPT's responses and found that it seldom failed to adhere to the expected JSON structure. In the rare case that malformed output is produced, the pipeline catches the parsing error and automatically reprompts GPT. Only one synthetic home failed generation, 0.403% of the attempted homes. An excerpt from an example GeoJSON object is provided in Figure 6.

3.4 Running EnergyPlus Simulations

To execute a simulation in EnergyPlus, we take the GeoJSON generated by GPT (Section 3.3) and convert it to an IDF file for use in EnergyPlus. We use a template IDF file, filled with default values that are replaced with variables from the GeoJSON data, such as the geometry, HVAC heating and cooling coefficients of performance and R-values for the wall and roof. Additionally, the template has many fields with constant values, such as the simulation running period and materials, constructions, and zones used in the simulation. Once the details from the GeoJSON are copied into the template, a final IDF file is produced.

The templating process is facilitated with the `eppy` package (santoshphilip 2024), which makes programmatic IDF generation straightforward. Then, we use ExpandObjects to prepare the file for simulation. ExpandObjects is bundled with EnergyPlus, and its primary use case is to take an IDF and expand template objects—such as the `HVACTemplate` we use—into full systems (U.S. Department of Energy 2023). Finally, we run the expanded IDF file through EnergyPlus, producing final simulation results.

We write the inspection notes and EnergyPlus simulation results for each example into one JSON Lines (JSONL) file. This completes our end-to-end dataset generation process, yielding a unified dataset that combines textual and simulation-based information.

4 Validating Plausibility of Pipeline Generated Data

Following prior work on synthetic data evaluation (Patki et al. 2016; Goncalves et al. 2020; Du and N. Li 2025; Lautrup et al. 2024), we view synthetic data plausibility as application dependent, linked to the properties of the domain in focus rather than as a single universal mechanism to validate data across all domains. Given that the purpose of our framework is to generate simulation-ready residential building models and in this field there is not an agreed validation approach for such synthetic data, we utilize interval coverage metrics to evaluate the empirical plausibility of our generated data.

Interval coverage metrics are widely used to evaluate whether model outputs remain within statistically expected ranges (Krüger and Plett 2024; Schmidinger and Heuvelink 2023). Krüger and Plett (2024) use interval coverage as a principal measure of interval calibration, whereas Schmidinger and Heuvelink (2023) evaluate coverage alongside complementary uncertainty metrics. Furthermore, percentile distributions have been used as part of the evaluation of synthetic building-energy profiles (Patidar et al. 2016). Drawing on these complementary evaluation perspectives, we define plausible reference intervals of the corresponding ResStock (Present et al. 2024; Reyna et al. 2025) variables and evaluate the proportion of generated values that fall within these intervals. ResStock is a publicly available dataset developed by the U.S. Department of Energy to represent the U.S. residential building stock. The selected interval, the 10th–90th percentiles, excludes the extreme tails of the empirical ResStock distribution while retaining its central region. The bottom of the interval was selected given that Patidar et al. (2016) leave the 0th-10th percentiles out of their evaluation interval, and the top was selected for symmetry.

Our comparison is restricted to Climate Zone 4A and to the four variables that vary across synthetic homes—Wall R-Value, Roof R-Value, Cooling COP, and Heating COP—because of their importance in building energy simulation. Each variable is evaluated separately against its corresponding ResStock reference interval. This reflects the objective of assessing the plausibility of individual generated building characteristics, including uncommon but physically plausible homes that need not conform to the joint distribution of the reference dataset. The remaining approximately 150 variables are fixed template values outside the generative pipeline, although the pipeline could readily be extended to generate these as well. The evaluation corpus consists of 247 synthetic homes and 2,000 ResStock Climate Zone 4A samples. In addition to the proposed plausibility coverage metric, we report statistics that provide descriptive context for both datasets.

Variable	Coverage (%)	ResStock Q1–Q3	Synthetic Mean	Synthetic Median
Wall R-Value	98.38	1.94–2.64	2.42	2.29
Roof R-Value	100.0	3.35–6.69	5.21	5.28
Cooling COP	58.70	3.1–3.8	2.90	3.00
Heating COP	99.59	0.8–1.0	0.82	0.85

Table 4. Coverage of synthetic homes within the ResStock 10th–90th percentile interval for each variable, together with the ResStock interquartile range (Q1–Q3) and the synthetic homes mean and median.

Table 4 reports the plausibility coverage results for the four variables across all synthetic homes by displaying the percentage of values that fall within the ResStock 10th–90th percentile interval. We observed coverage greater than 58% for all variables and greater than 95% for three of the four variables. Under our coverage-based definition of plausibility, these results suggest that the generated values for these variables are largely consistent with the typical ranges observed in the reference dataset. Additionally, the table reports summary statistics for both datasets, including the mean and median of each variable for the synthetic homes and the interquartile range (IQR) observed in ResStock. These statistics are provided for descriptive context and are not used when computing the plausibility coverage metric.

Compared to prior generative urban-energy workflows, our framework incorporates both multimodal sensitivity analysis and reference-based plausibility validation against a national reference dataset. Occlusion provides empirical evidence that the image processing component of the pipeline behaves as intended. We additionally show that the generated variables generally fall within the empirically plausible reference intervals derived from ResStock, with coverage exceeding 95% for three of the four evaluated variables. While concerns regarding hallucinations and reliability remain important when using LLMs, the results presented here indicate that the proposed safeguards and validation procedures help mitigate some of the issues identified by M. Liu et al. (2025).

5 Conclusion

In this work, we presented a multimodal framework for generating simulation-ready synthetic residential data from public records, imagery by applying generative AI models. The results demonstrate the feasibility of generating simulation-ready synthetic residential data when comprehensive real-world data are unavailable. To the best of our knowledge, no prior approach has combined these heterogeneous data sources into a unified pipeline capable of producing both structured simulation inputs and complementary textual descriptions for residential buildings.

The proposed pipeline produces both structured building-energy models and accompanying textual descriptions, enabling the creation of dual-modality datasets suitable for simulation and downstream machine learning applications. To evaluate the reliability of the generated outputs, we introduced a validation framework that combines multimodal sensitivity analysis, structured-output verification, and plausibility-oriented comparison against a national reference dataset. Together, these analyses provide evidence that the generated homes are physically plausible, simulation compatible, and aligned with the intended objectives of the pipeline.

Recent reviews have highlighted the growing relevance of generative AI in building energy research while also identifying challenges related to reliability, validation, and practical deployment, motivating the development of robust methods for energy simulation workflows (H. Xu et al. 2024; M. Liu et al. 2025). The framework presented in this work contributes to this emerging area by providing a flexible approach for generating simulation-ready residential data under conditions of limited data availability. Beyond its

use for synthetic home generation, the framework may support a variety of downstream applications and can be extended in several directions. One particularly promising avenue for future work is the use of the generated data to support the training of machine learning models for urban energy applications. For instance, the pipeline could be expanded to utilize the resulting simulation data and inspection notes to label the efficiency of particular components that affect the energy efficiency of a home. These labeled homes could be used to train an ML model that provide recommendations for energy efficiency retrofits. Furthermore, such a model could help prioritize retrofit interventions for residential buildings. Moreover, such downstream use would complement the validation presented in this work by displaying the dataset's usefulness for predictive modeling.

Overall, this work evaluates plausibility, simulation compatibility, and task-aligned multimodal sensitivity, which align with the intended use of the generated homes as simulation-ready synthetic residential data. Rather than reconstructing ground-truth building geometries or calibrated utility measurements, the pipeline is designed to produce physically plausible and operationally useful representations under conditions of limited real-world data availability. Constructing large-scale authoritative datasets that satisfy realism constraints remains a broader challenge in residential energy modeling and synthetic urban data generation.

Ultimately, the high cost, limited availability, and privacy concerns associated with collecting urban energy data motivate the use of synthetic alternatives. Our framework helps address these data-access challenges by producing simulation-ready synthetic data accompanied by plausibility-oriented validation. By reducing dependence on costly or restricted data sources, the approach will broaden access to data-driven research in the urban energy domain.

Acknowledgments

The authors extend gratitude to Lafayette College for supporting this work by funding it through the EXCEL Scholars program and providing computational resources with the Firebird high performance computing cluster. Access to the JetStream2 system was made possible via the NSF-funded ACCESS program, facilitated by Lafayette College. We also thank the NSF and ACCESS for supporting this resource, and Indiana University for hosting JetStream2 as a part of the ACCESS program.

CRediT Author Attributions

Jackson Eshbaugh: Software, Investigation, Writing - Original Draft, Visualization, Validation, Data Curation. **Chetan Tiwari**: Conceptualization, Writing - Review and Editing, Supervision (supporting). **Jorge Silveyra**: Conceptualization, Writing - Review and Editing, Methodology, Supervision (lead), Project Administration, Validation

Glossary

EnergyPlus A versatile building energy modeling tool provided by the United States Department of Energy. Originally published in 2002.

GPT A popular large language model by OpenAI with a wide variety of uses.

LLaVA An LLM integrated with CLIP, OpenAI's visual model. Introduced by Liu *et al.* in 2023.

Occlusion A test commonly used to evaluate visual machine learning models by blocking out parts of an image and comparing to a baseline.

Acronyms

AI Artificial Intelligence

GeoJSON Geographic JSON

IDF Input Definition File

JSON JavaScript Object Notation
JSONL JSON Lines

LLM Large Language Model

ML Machine Learning

References

Agostinelli, S., F. Cumo, G. Guidi, and C. Tomazzoli (Apr. 2021). Cyber-Physical Systems Improving Building Energy Management: Digital Twin and Artificial Intelligence. In: *Energies* 14.8, p. 2338. DOI: 10.3390/en14082338. (Visited on 07/28/2025).

Ansel, J., E. Yang, H. He, N. Gimelshein, A. Jain, M. Voznesensky, B. Bao, P. Bell, D. Berard, E. Burovski, G. Chauhan, A. Chourdia, W. Constable, A. Desmaison, Z. DeVito, E. Ellison, W. Feng, J. Gong, M. Gschwind, B. Hirsh, S. Huang, K. Kalambarkar, L. Kirsch, M. Lazos, M. Lezcano, Y. Liang, J. Liang, Y. Lu, C. K. Luk, B. Maher, Y. Pan, C. Puhrsch, M. Reso, M. Saroufim, M. Y. Siraichi, H. Suk, S. Zhang, M. Suo, P. Tillet, X. Zhao, E. Wang, K. Zhou, R. Zou, X. Wang, A. Mathews, W. Wen, G. Chanan, P. Wu, and S. Chintala (Apr. 2024). PyTorch 2: Faster Machine Learning Through Dynamic Python Bytecode Transformation and Graph Compilation. In: *Proceedings of the 29th ACM International Conference on Architectural Support for Programming Languages and Operating Systems, Volume 2*. La Jolla CA USA: ACM, pp. 929–947. DOI: 10.1145/3620665.3640366. (Visited on 07/31/2025).

Balkir, E., I. Nejadgholi, K. Fraser, and S. Kiritchenko (2022). Necessity and Sufficiency for Explaining Text Classifiers: A Case Study in Hate Speech Detection. In: *Proceedings of the 2022 Conference of the North American Chapter of the Association for Computational Linguistics: Human Language Technologies*. Seattle, United States: Association for Computational Linguistics, pp. 2672–2686. DOI: 10.18653/v1/2022.naacl-main.192. (Visited on 07/28/2025).

Belik, M. and O. Rubanenko (June 2023). Implementation of Digital Twin for Increasing Efficiency of Renewable Energy Sources. In: *Energies* 16.12, p. 4787. DOI: 10.3390/en16124787. (Visited on 07/28/2025).

Bishop, D., P. Gallardo, and B. L. M. Williams (2024). A Review of Multi-Domain Urban Energy Modelling Data. In: *Clean Energy and Sustainability* 2.4, pp. 10016–10016. DOI: 10.70322/ces.2024.10016. URL: https://www.sciepublish.com/article/pii/298 (visited on 08/16/2025).

Bompard, E. F., S. Conti, M. J. Masera, and G. G. Soma (Nov. 2024). A New Electricity Infrastructure for Fostering Urban Sustainability: Challenges and Emerging Trends. In: *Energies* 17.22, p. 5573. DOI: 10.3390/en17225573. (Visited on 08/12/2025).

Crawley, D. B., L. K. Lawrie, F. C. Winkelmann, W. Buhl, Y. Huang, C. O. Pedersen, R. K. Strand, R. J. Liesen, D. E. Fisher, M. J. Witte, and J. Glazer (Apr. 2001). EnergyPlus: Creating a New-Generation Building Energy Simulation Program. In: *Energy and Buildings* 33.4, pp. 319–331. DOI: 10.1016/S0378-7788(00)00114-6. (Visited on 07/28/2025).

Dodge, S., J. Xu, and B. Stenger (May 2017). Parsing Floor Plan Images. In: *2017 Fifteenth IAPR International Conference on Machine Vision Applications (MVA)*. Nagoya, Japan: IEEE, pp. 358–361. DOI: 10.23919/MVA.2017.7986875. (Visited on 07/31/2025).

Du, Y. and N. Li (2025). Systematic Assessment of Tabular Data Synthesis. In: *Proceedings of the 2025 ACM SIGSAC Conference on Computer and Communications Security*. CCS '25. Taipei, Taiwan: Association for Computing Machinery, pp. 2414–2428. DOI: 10.1145/3719027.3765067. URL: https://doi.org/10.1145/3719027.3765067.

Elnabawi, M. H. and N. Hamza (Sept. 2022). A Methodology of Creating a Synthetic, Urban-Specific Weather Dataset Using a Microclimate Model for Building Energy Modelling. In: *Buildings* 12.9, p. 1407. DOI: 10.3390/buildings12091407. (Visited on 07/28/2025).

Francisco, A., N. Mohammadi, and J. E. Taylor (Mar. 2020). Smart City Digital Twin–Enabled Energy Management: Toward Real-Time Urban Building Energy Benchmarking. In: *Journal of Management in Engineering* 36.2, p. 04019045. DOI: 10.1061/(ASCE)ME.1943-5479.0000741. (Visited on 07/28/2025).

Goncalves, A., P. Ray, B. Soper, J. Stevens, L. Coyle, and A. P. Sales (May 2020). Generation and Evaluation of Synthetic Patient Data. In: *BMC Medical Research Methodology* 20.1, p. 108. DOI: 10.1186/s12874-020-00977-1.

Google (June 2023). *ChromeDriver - WebDriver for Chrome*. https://sites.google.com/chromium.org/driver/. Accessed: 2025-08-06.

Guo, T., M. Bachmann, M. Kersten, and M. Kriegel (Sept. 2023). A Combined Workflow to Generate Citywide Building Energy Demand Profiles from Low-Level Datasets. In: *Sustainable Cities and Society* 96, p. 104694. DOI: 10.1016/j.scs.2023.104694. URL: https://linkinghub.elsevier.com/retrieve/pii/S2210670723003050 (visited on 08/16/2025).

Hajri, A., R. Garay-Marinez, A. M. Macarulla, and M. A. Ben Sassi (Aug. 2025). Data-Driven Model for Heat Load Prediction in Buildings Connected to District Heating Networks. In: *Energy* 329, p. 136684. DOI: 10.1016/j.energy.2025.136684. (Visited on 09/10/2025).

Hooker, S., D. Erhan, P.-J. Kindermans, and B. Kim (Nov. 2019). *A Benchmark for Interpretability Methods in Deep Neural Networks*. DOI: 10.48550/arXiv.1806.10758. arXiv: 1806.10758 [cs]. (Visited on 07/28/2025).

Janssens, A. C. J. W. and F. K. Martens (Aug. 2020). Reflection on Modern Methods: Revisiting the Area under the ROC Curve. In: *International Journal of Epidemiology* 49.4, pp. 1397–1403. DOI: 10.1093/ije/dyz274. (Visited on 07/31/2025).

Krüger, F. and H. Plett (Sept. 2024). Prediction Intervals for Economic Fixed-Event Forecasts. In: *The Annals of Applied Statistics* 18.3. DOI: 10.1214/24-AOAS1900. (Visited on 07/07/2026).

Lautrup, A. D., T. Hyrup, A. Zimek, and P. Schneider-Kamp (Dec. 2024). SynthEval: A Framework for Detailed Utility and Privacy Evaluation of Tabular Synthetic Data. In: *Data Mining and Knowledge Discovery* 39.1, p. 6. DOI: 10.1007/s10618-024-01081-4.

Lee, S., J. Cha, M. K. Kim, K. S. Kim, V. H. Pham, and M. Leach (Oct. 2019). Neural-Network-Based Building Energy Consumption Prediction with Training Data Generation. In: *Processes* 7.10, p. 731. DOI: 10.3390/pr7100731. (Visited on 07/28/2025).

Li, J., D. Li, S. Savarese, and S. Hoi (June 2023). *BLIP-2: Bootstrapping Language-Image Pre-training with Frozen Image Encoders and Large Language Models*. DOI: 10.48550/arXiv.2301.12597. arXiv: 2301.12597 [cs]. (Visited on 08/29/2025).

Lin, Y., Y. Yao, J. Zhu, and C. He (Mar. 2025). Application of Generative AI in Predictive Analysis of Urban Energy Distribution and Traffic Congestion in Smart Cities. In: *2025 IEEE International Conference on Electronics, Energy Systems and Power Engineering (EESPE)*. Shenyang, China: IEEE, pp. 765–768. DOI: 10.1109/EESPE63401.2025.10987500. (Visited on 07/31/2025).

Liu, H., C. Li, Y. Li, and Y. J. Lee (June 2024). Improved Baselines with Visual Instruction Tuning. In: *2024 IEEE/CVF Conference on Computer Vision and Pattern Recognition (CVPR)*. Seattle, WA, USA: IEEE, pp. 26286–26296. DOI: 10.1109/CVPR52733.2024.02484. (Visited on 05/26/2026).

Liu, H., C. Li, Q. Wu, and Y. J. Lee (Dec. 2023). *Visual Instruction Tuning*. DOI: 10.48550/arXiv.2304.08485. arXiv: 2304.08485 [cs]. (Visited on 07/28/2025).

Liu, M., L. Zhang, J. Chen, W.-A. Chen, Z. Yang, L. J. Lo, J. Wen, and Z. O'Neill (Feb. 2025). Large Language Models for Building Energy Applications: Opportunities and Challenges. In: *Building Simulation* 18.2, pp. 225–234. DOI: 10.1007/s12273-025-1235-9. (Visited on 07/31/2025).

OpenAI (Apr. 2025). *Introducing GPT-4.1 in the API*. https://openai.com/index/gpt-4-1/. (Visited on 07/31/2025).

Patidar, S., D. Jenkins, and S. Simpson (Sept. 2016). Stochastic modelling techniques for generating synthetic energy demand profiles. In: *International Journal of Energy and Statistics* 4, p. 1650014. DOI: 10.1142/S2335680416500149.

Patki, N., R. Wedge, and K. Veeramachaneni (2016). The Synthetic Data Vault. In: *2016 IEEE International Conference on Data Science and Advanced Analytics (DSAA)*, pp. 399–410. DOI: 10.1109/DSAA.2016.49.

Perera, A., K. Javanroodi, and V. M. Nik (Mar. 2021). Climate Resilient Interconnected Infrastructure: Co-optimization of Energy Systems and Urban Morphology. In: *Applied Energy* 285, p. 116430. DOI: 10.1016/j.apenergy.2020.116430. (Visited on 08/12/2025).

Present, E., P. R. White, C. Harris, R. Adhikari, Y. Lou, L. Liu, A. Fontanini, C. Moreno, J. Robertson, and J. Maguire (2024). *ResStock 2024.1 Dataset*. ResStock 2024.1 dataset. DOI: 10.2172/2319195. URL: https://doi.org/10.2172/2319195.

Radford, A., J. W. Kim, C. Hallacy, A. Ramesh, G. Goh, S. Agarwal, G. Sastry, A. Askell, P. Mishkin, J. Clark, G. Krueger, and I. Sutskever (Feb. 2021). *Learning Transferable Visual Models From Natural Language Supervision*. DOI: 10.48550/arXiv.2103.00020. arXiv: 2103.00020 [cs]. (Visited on 08/29/2025).

Rehmann, F., M. Mosteiro-Romero, C. Miller, and R. Streblow (Nov. 2025). Enhancing Urban Energy Modeling: A Case Study of Data Acquisition, Enrichment, and Evaluation in Berlin. In: *Energy and Buildings* 346, p. 116070. DOI: 10.1016/j.enbuild.2025.116070. URL: https://linkinghub.elsevier.com/retrieve/pii/S037877882500800X (visited on 08/16/2025).

Reimers, N. and I. Gurevych (Aug. 2019). *Sentence-BERT: Sentence Embeddings Using Siamese BERT-Networks*. DOI: 10.48550/arXiv.1908.10084. arXiv: 1908.10084 [cs]. (Visited on 08/06/2025).

Reyna, J., A. Fontanini, E. Present, L. Liu, R. Adhikari, C. Bianchi, J. Brossman, R. Chintala, K. Clark, C. Harris, S. Horowitz, Y. Lou, J. Maguire, N. Merket, N. Moore, P. Munankarmi, J. Robertson, N. Sandoval, A. Speake, K. Stenger, P. White, and E. Wilson (2025). *ResStock Technical Reference Documentation v3.3.0*. ResStock Technical Reference Documentation. DOI: 10.2172/2583488. URL: https://doi.org/10.2172/2583488.

santoshphilip (Oct. 2024). *Eppy*. https://github.com/santoshphilip/eppy. (Visited on 08/07/2025).

Schmidinger, J. and G. B. Heuvelink (2023). Validation of uncertainty predictions in digital soil mapping. In: *Geoderma* 437, p. 116585. DOI: https://doi.org/10.1016/j.geoderma.2023.116585. URL: https://www.sciencedirect.com/science/article/pii/S0016706123002628.

Selenium (Nov. 2024). *Selenium WebDriver Documentation*. https://www.selenium.dev/documentation/webdriver/. Accessed 2025-08-06.

Sha, Z., W. Yue, S. Wang, N. Cheng, J. Wu, and C. Li (June 2024). Generative AI-Enabled Sensing and Communication Integration for Urban Air Mobility. In: *2024 IEEE 99th Vehicular Technology Conference (VTC2024-Spring)*. Singapore, Singapore: IEEE, pp. 1–5. DOI: 10.1109/VTC2024-Spring62846.2024.10683276. (Visited on 07/31/2025).

Shorten, C., C. Pierse, T. B. Smith, E. Cardenas, A. Sharma, J. Trengrove, and B. van Luijt (Aug. 2024). *StructuredRAG: JSON Response Formatting with Large Language Models*. DOI: 10.48550/arXiv.2408.11061. arXiv: 2408.11061 [cs]. (Visited on 08/06/2025).

Stinner, F., M. Wiecek, M. Baranski, A. Kümpel, and D. Müller (Aug. 2021). *Automatic Digital Twin Data Model Generation of Building Energy Systems from Piping and Instrumentation Diagrams*. DOI: 10.48550/arXiv.2108.13912. arXiv: 2108.13912 [cs]. (Visited on 07/28/2025).

The Matplotlib Development Team (May 2025). *Matplotlib: Visualization with Python*. Zenodo. DOI: 10.5281/ZENODO.15375714. (Visited on 08/01/2025).

Tyler Technologies (July 2022). *Orange County, Florida, Selects Enterprise Assessment & Tax Solution from Tyler Technologies*. Tyler Technologies. URL: https://investors.tylertech.com/news/news-details/2022/Orange-County-Florida-Selects-Enterprise-Assessment--Tax-Solution-from-Tyler-Technologies/default.aspx (visited on 05/27/2026).

U.S. Department of Energy (2023). *EnergyPlus Auxiliary Programs Documentation — Version 23.2.0*. See pages 45–48 for `ExpandObjects` preprocessor details. EnergyPlus, U.S. Department of Energy. URL: https://energyplus.net/assets/nrel_custom/pdfs/pdfs_v23.2.0/AuxiliaryPrograms.pdf.

— (Mar. 2025). *Getting Started*. URL: https://energyplus.net/assets/nrel_custom/pdfs/pdfs_v25.1.0/GettingStarted.pdf (visited on 08/15/2025).

U.S. Energy Information Administration (May 2025). *After more than a decade of little change, U.S. electricity consumption is rising again*. https://www.eia.gov/todayinenergy/detail.php?id=65264.

U.S. Environmental Protection Agency (Jan. 2025). *Climate Change Indicators: Residential Energy Use*. https://www.epa.gov/climate-indicators/climate-change-indicators-residential-energy-use. Reports and Assessments. (Visited on 08/12/2025).

Wan, D., X. Zhao, W. Lu, P. Li, X. Shi, and H. Fukuda (July 2022). A Deep Learning Approach toward Energy-Effective Residential Building Floor Plan Generation. In: *Sustainability* 14.13, p. 8074. DOI: 10.3390/su14138074. (Visited on 07/28/2025).

Wolf, T., L. Debut, V. Sanh, J. Chaumond, C. Delangue, A. Moi, P. Cistac, T. Rault, R. Louf, M. Funtowicz, J. Davison, S. Shleifer, P. Von Platen, C. Ma, Y. Jernite, J. Plu, C. Xu, T. Le Scao, S. Gugger, M. Drame, Q. Lhoest, and A. Rush (2020). Transformers: State-of-the-Art Natural Language Processing. In: *Proceedings of the 2020 Conference on Empirical Methods in Natural Language Processing: System Demonstrations*. Online: Association for Computational Linguistics, pp. 38–45. DOI: 10.18653/v1/2020.emnlp-demos.6. (Visited on 07/31/2025).

Xiao, T. and P. Xu (Nov. 2024). Exploring Automated Energy Optimization with Unstructured Building Data: A Multi-Agent Based Framework Leveraging Large Language Models. In: *Energy and Buildings* 322, p. 114691. DOI: 10.1016/j.enbuild.2024.114691. (Visited on 07/31/2025).

Xu, H., F. Omitaomu, S. Sabri, S. Zlatanova, X. Li, and Y. Song (Oct. 2024). Leveraging Generative AI for Urban Digital Twins: A Scoping Review on the Autonomous Generation of Urban Data, Scenarios, Designs, and 3D City Models for Smart City Advancement. In: *Urban Informatics* 3.1, p. 29. DOI: 10.1007/s44212-024-00060-w. (Visited on 07/28/2025).

Yang, Z., L. Li, K. Lin, J. Wang, C.-C. Lin, Z. Liu, and L. Wang (Oct. 2023). *The Dawn of LMMs: Preliminary Explorations with GPT-4V(Ision)*. DOI: 10.48550/arXiv.2309.17421. arXiv: 2309.17421 [cs]. (Visited on 08/29/2025).

Zeng, Y., Y. Cai, G. Huang, and J. Dai (Oct. 2011). A Review on Optimization Modeling of Energy Systems Planning and GHG Emission Mitigation under Uncertainty. In: *Energies* 4.10, pp. 1624–1656. DOI: 10.3390/en4101624. (Visited on 08/12/2025).

Zhang, L., V. Ford, Z. Chen, and J. Chen (Jan. 2025). Automatic Building Energy Model Development and Debugging Using Large Language Models Agentic Workflow. In: *Energy and Buildings* 327, p. 115116. DOI: 10.1016/j.enbuild.2024.115116. (Visited on 09/12/2025).

Zhang, S., Q. Fang, Z. Yang, and Y. Feng (Mar. 2025). *LLaVA-Mini: Efficient Image and Video Large Multimodal Models with One Vision Token*. DOI: 10.48550/arXiv.2501.03895. arXiv: 2501.03895 [cs]. (Visited on 08/29/2025).

Zhang, Y., A. Schlüter, and C. Waibel (June 2022). *SolarGAN: Synthetic Annual Solar Irradiance Time Series on Urban Building Facades via Deep Generative Networks*. DOI: 10.48550/arXiv.2206.00747. arXiv: 2206.00747 [cs]. (Visited on 07/31/2025).

Zhu, D., J. Chen, X. Shen, X. Li, and M. Elhoseiny (Oct. 2023). *MiniGPT-4: Enhancing Vision-Language Understanding with Advanced Large Language Models*. DOI: 10.48550/arXiv.2304.10592. arXiv: 2304.10592 [cs]. (Visited on 08/29/2025).

Zweig, M. H. and G. Campbell (Apr. 1993). Receiver-Operating Characteristic (ROC) Plots: A Fundamental Evaluation Tool in Clinical Medicine. In: *Clinical Chemistry* 39.4, pp. 561–577. DOI: 10.1093/clinchem/39.4.561. (Visited on 07/31/2025).

A Occlusion Results

In this appendix, we provide detailed information and results from our occlusion tests. Firstly, when running the test we utilized identical prompts for each model. For GPT, we prompted:

> You are a certified home inspector. Describe the status roof. Is it in good condition? Why or why not?

Likewise, we prompted LLaVA with the following:

> USER: <image>
> You are a certified home inspector. Describe the status roof. Is it in good condition? Why or why not? ASSISTANT:

These prompts differ slightly due to how the models are trained; namely, LLaVA expects an image token and labeled portions of the message. The majority of LLMs behave this way, and the GPT API likely wraps the given prompt in something similar.

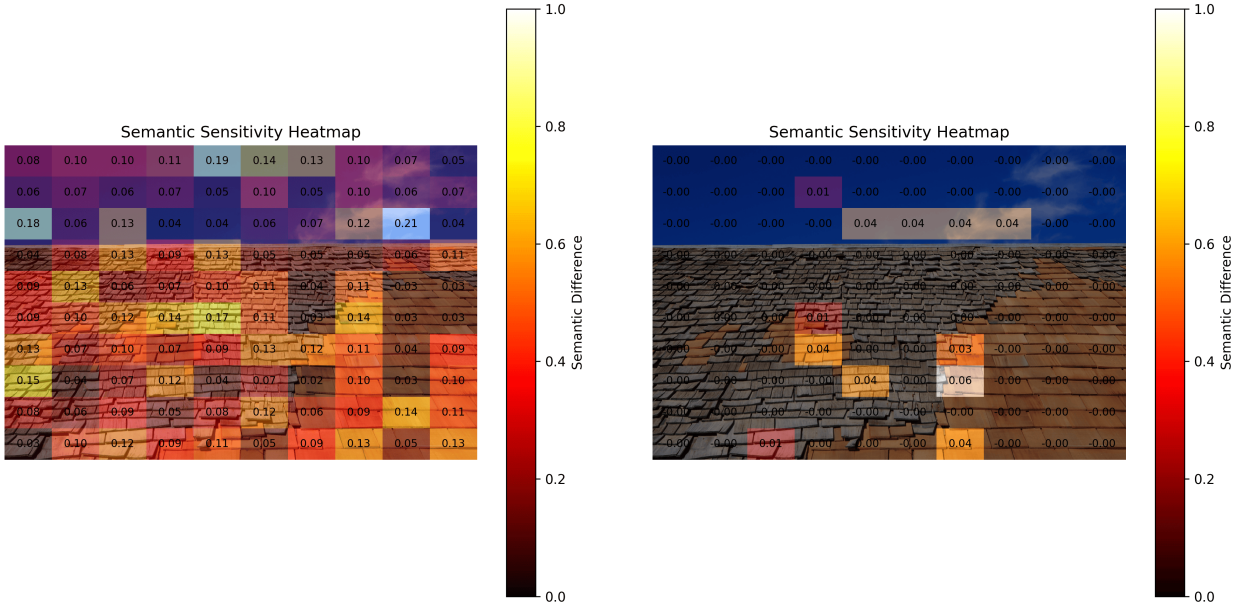
Next, we provide our hypotheses pertaining to the performance of both models. We hypothesize that LLaVA's advantage stems from its architecture: it employs an early fusion design in which images are converted into visual tokens by CLIP (Radford et al. 2021) that are then prepended to the textual prompt (H. Liu, C. Li, Wu, et al. 2023). These visual tokens are passed through the transformer layers of the LLM together with text tokens, enabling multimodal attention at every layer. It has been demonstrated that vision tokens are most critical for a model in early layers, when they fuse into text tokens (S. Zhang et al. 2025). A likely result of this is the reduction of the model's sensitivity to variations in the image, which may explain its stronger performance in our experiments.

While GPT-4V (GPT's vision model) is proprietary, the case can be made that it possesses a different structure. Evaluation studies show that it performs well across visual reasoning and captioning tasks, but it falls short in fine grained visual problems, requiring complex visual tasks to be broken up into interleaved subfigures and text (Yang et al. 2023). These evaluations are similar to evaluations from late fusion (connector) models. For example, BLIP-2 shows strengths in captioning images and instruction-following, while it is less robust with fine-grained spatial reasoning (J. Li et al. 2023). Another model, MiniGPT-4, demonstrates a similar profile: it has strengths in tasks such as image description, but falters with complex spatial reasoning (Zhu et al. 2023). Both BLIP-2 and MiniGPT-4 are late fusion models, where compressed visual features are routed into the LLM at later stages (J. Li et al. 2023; Zhu et al. 2023). As shown, BLIP-2, MiniGPT-4, and GPT-4V all suffer from a very similar weakness: fine-grained or complex spatial reasoning. Based on this similarity, we hypothesize that GPT-4V is also a late fusion model. This helps explain why GPT performed differently from LLaVA in our experiments: as structure dictates function, differences in behavior strongly suggest differences in design. On the basis of this analysis, we feel confident to select LLaVA to complete this task.

In Table 5, we provide our forward occlusion results, including roof mean difference (RMD) and non-roof mean difference (NRMD) values from both GPT and LLaVA and references to figures displaying GPT and LLaVA heatmaps side by side.

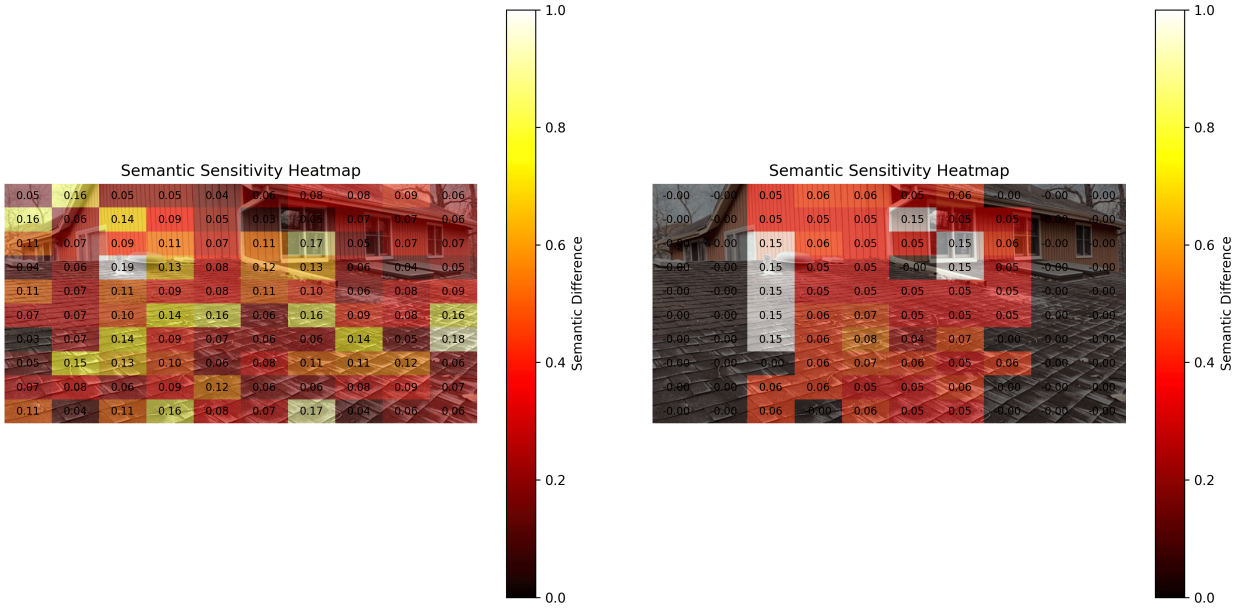
Metric	1	2	3	4	5	6	7	8	9	10
Damaged Roofs										
GPT RMD	0.0856	0.0920	0.0730	0.0689	0.1127	0.0453	0.0516	0.0603	0.1149	0.0419
GPT NRMD	0.0903	0.0745	0.0615	0.0824	0.0900	0.0375	0.0485	0.0900	0.1000	0.0442
LLaVA RMD	0.0033	0.0324	0.0949	0.0093	0.0262	0.0269	0.0356	0.0055	0.0038	0.0208
LLaVA NRMD	0.0057	0.0545	0.0723	0.0059	0.0200	0.0000	0.0335	0.0055	0.0022	0.0042
Roof Cells	70	80	53	83	97	96	80	96	91	88
Non-Roof Cells	30	20	47	17	3	4	20	4	9	12
Figure	7	8	9	10	11	12	13	14	15	16
Undamaged Roofs										
GPT RMD	0.1128	0.0785	0.1465	0.1508	0.0822	0.0956	0.1087	0.2005	0.0696	0.1200
GPT NRMD	0.1055	0.0742	0.1872	0.1598	0.0884	0.0930	0.1230	0.1898	0.0768	0.0959
LLaVA RMD	0.0709	0.0085	0.0007	0.0000	0.0340	0.0108	0.0066	0.0000	0.0017	0.0240
LLaVA NRMD	0.0313	0.0062	0.0000	0.0000	0.0321	0.0023	0.0030	0.0000	0.0015	0.0181
Roof Cells	53	47	68	49	81	39	70	60	47	73
Non-Roof Cells	47	53	32	51	19	61	30	40	53	27
Figure	17	18	19	20	21	22	23	24	25	26

Table 5. Quantitative results from our forward occlusion experiments, including roof mean difference (RMD) and non-roof mean difference (NRMD) for both GPT and LLaVA. The number of cells in the image considered roof and non-roof are listed, and figures of side by side comparisons of the resulting heatmaps are referenced.



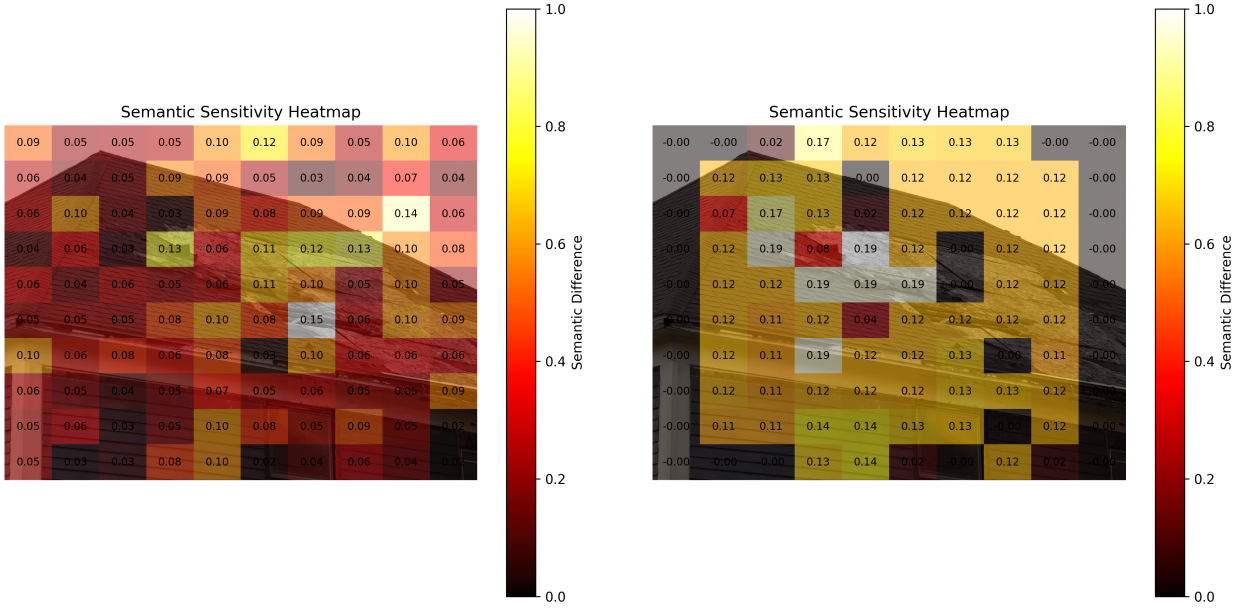
(a) GPT Heatmap **(b)** LLaVA Heatmap

Figure 7. Forward Occlusion—Damaged Roof 1



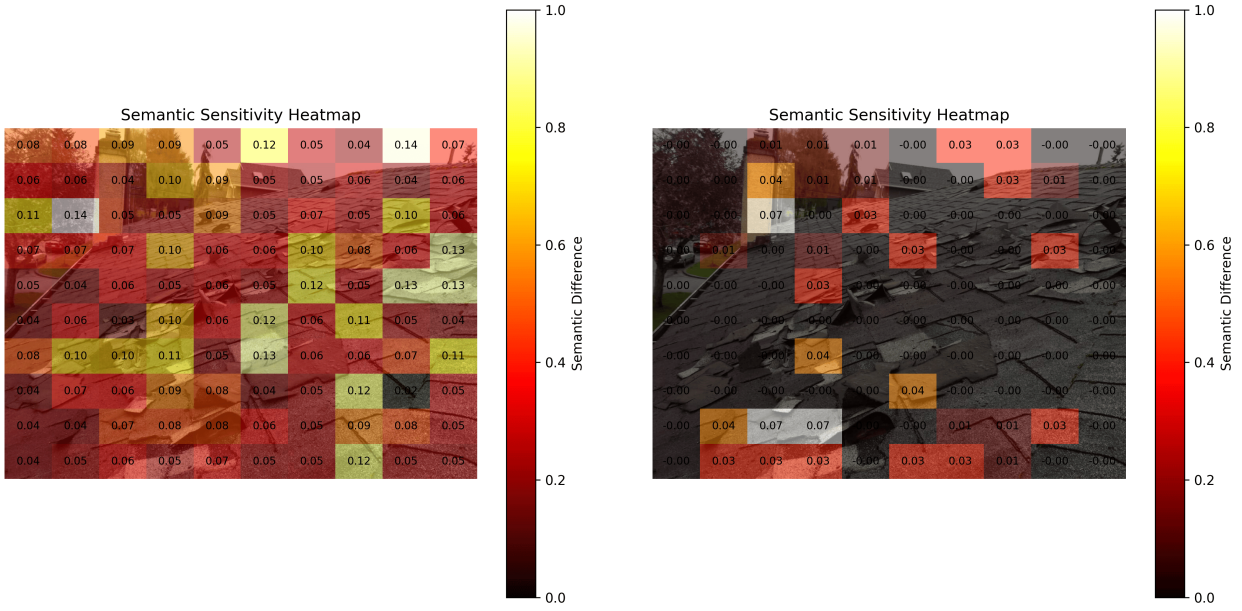
(a) GPT Heatmap **(b)** LLaVA Heatmap

Figure 8. Forward Occlusion—Damaged Roof 2



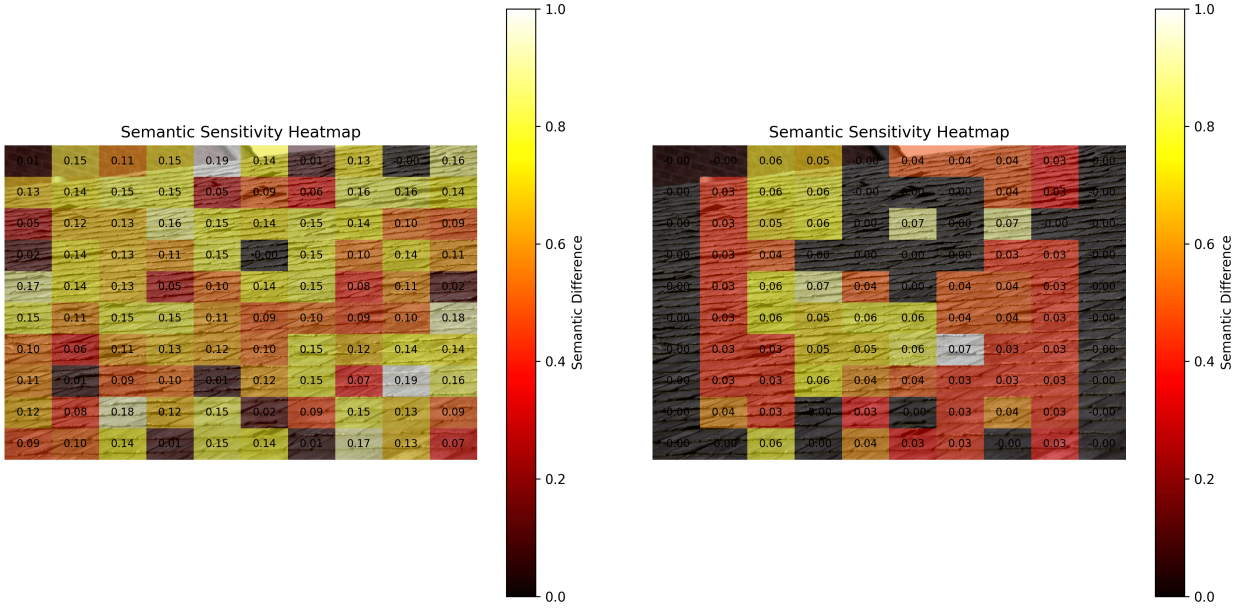
(a) GPT Heatmap **(b)** LLaVA Heatmap

Figure 9. Forward Occlusion—Damaged Roof 3



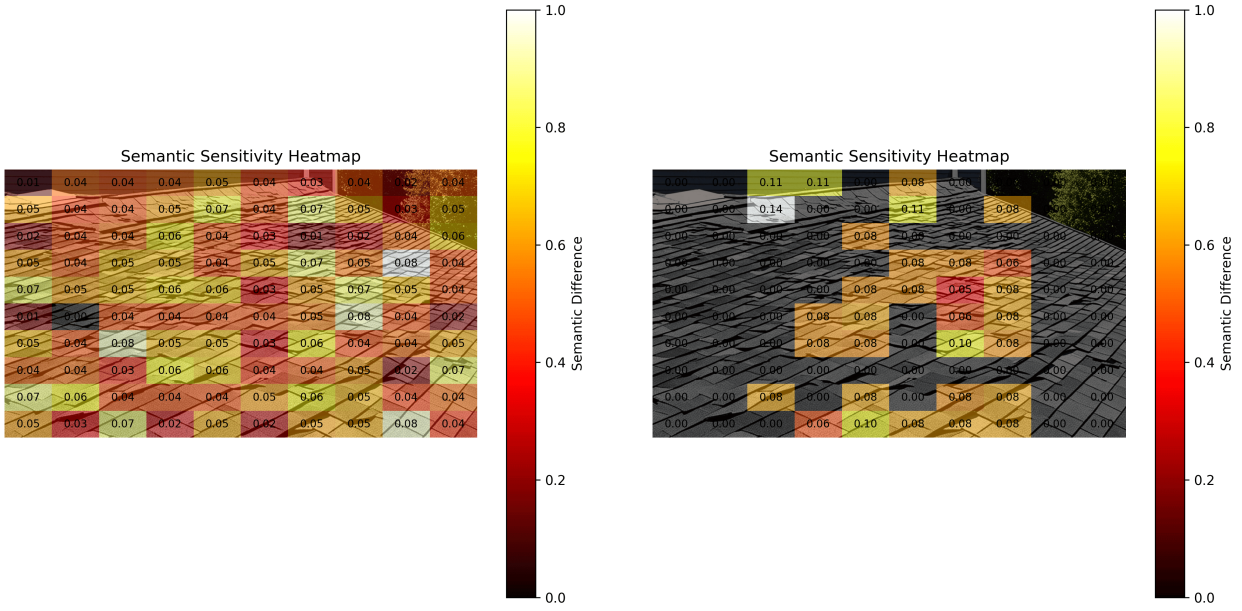
(a) GPT Heatmap **(b)** LLaVA Heatmap

Figure 10. Forward Occlusion—Damaged Roof 4



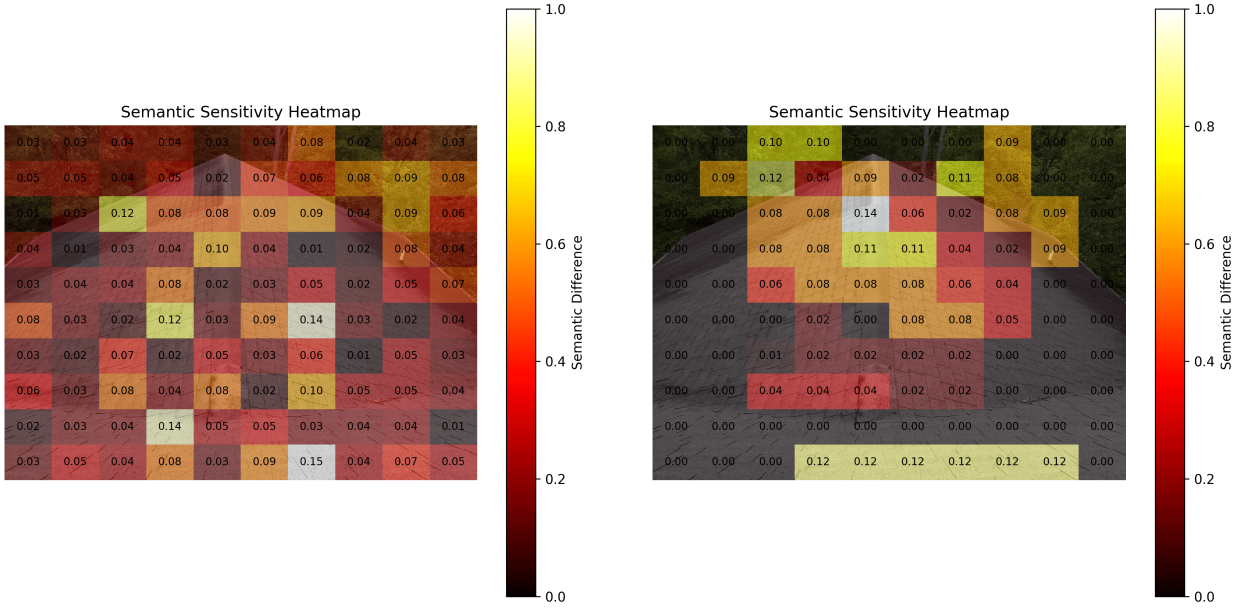
(a) GPT Heatmap **(b)** LLaVA Heatmap

Figure 11. Forward Occlusion—Damaged Roof 5



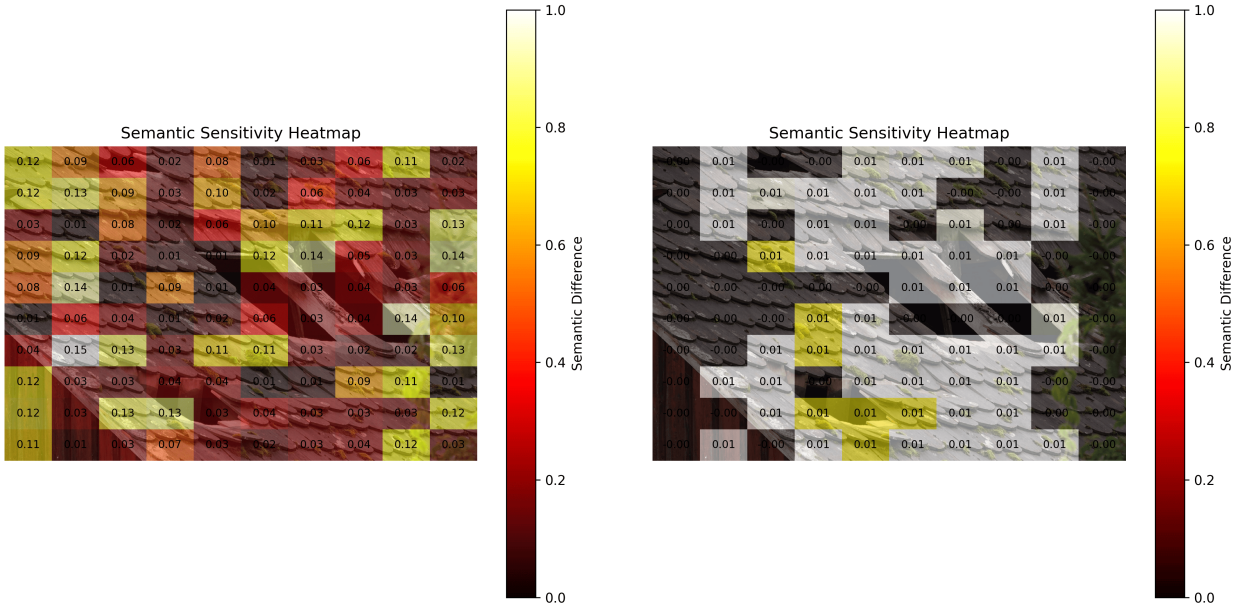
(a) GPT Heatmap **(b)** LLaVA Heatmap

Figure 12. Forward Occlusion—Damaged Roof 6



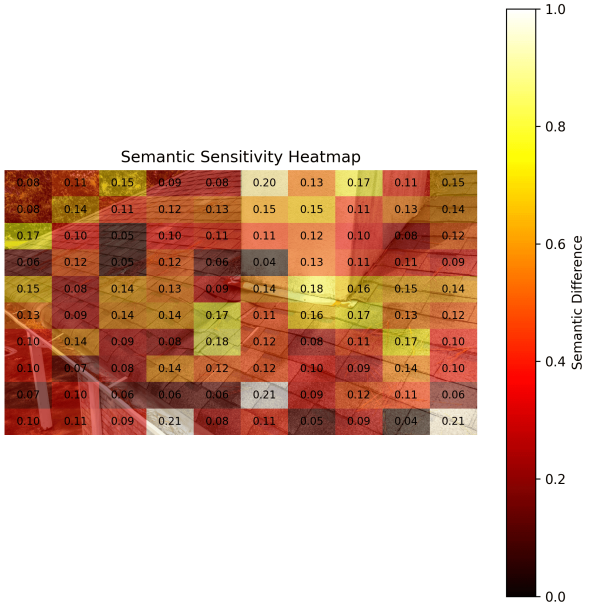
(a) GPT Heatmap **(b)** LLaVA Heatmap

Figure 13. Forward Occlusion—Damaged Roof 7

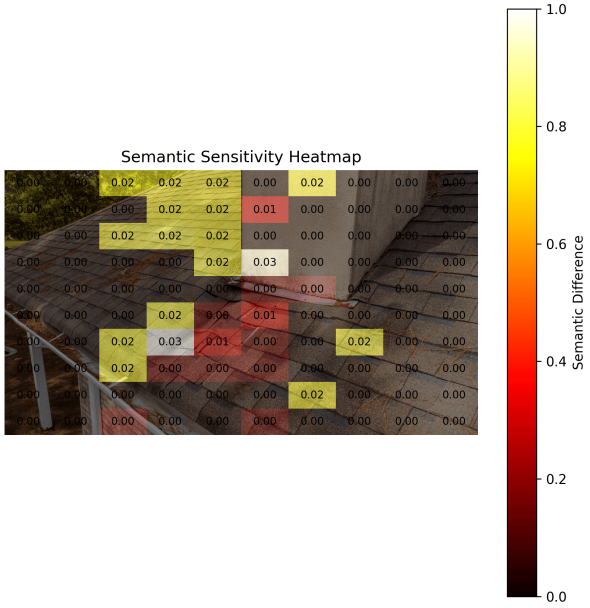


(a) GPT Heatmap **(b)** LLaVA Heatmap

Figure 14. Forward Occlusion—Damaged Roof 8

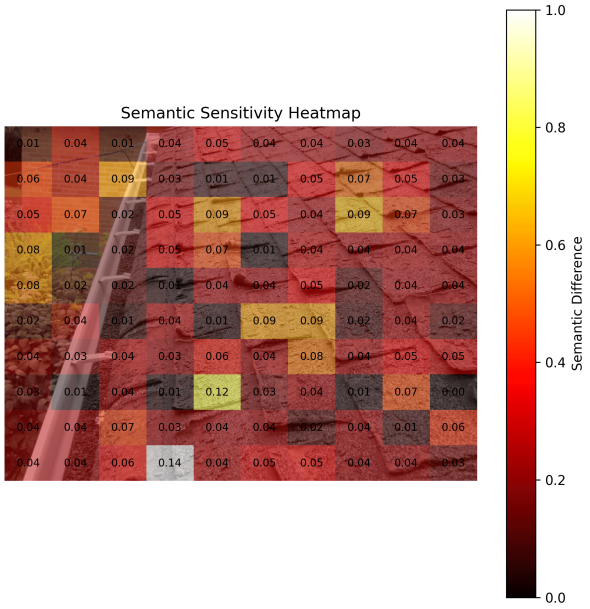


(a) GPT Heatmap

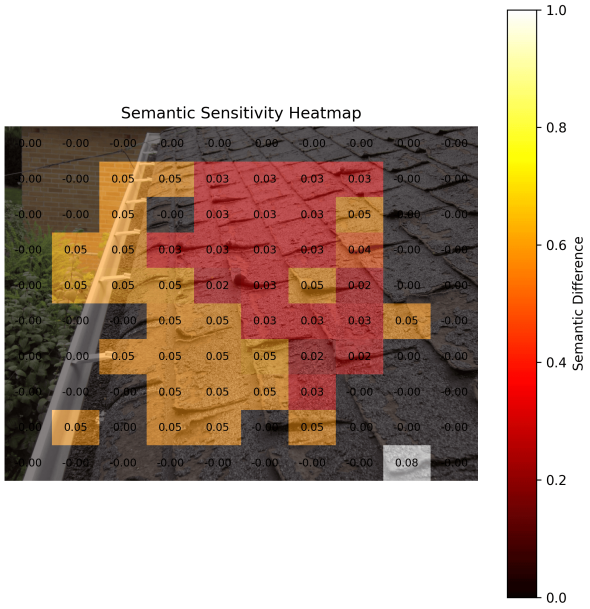


(b) LLaVA Heatmap

Figure 15. Forward Occlusion—Damaged Roof 9

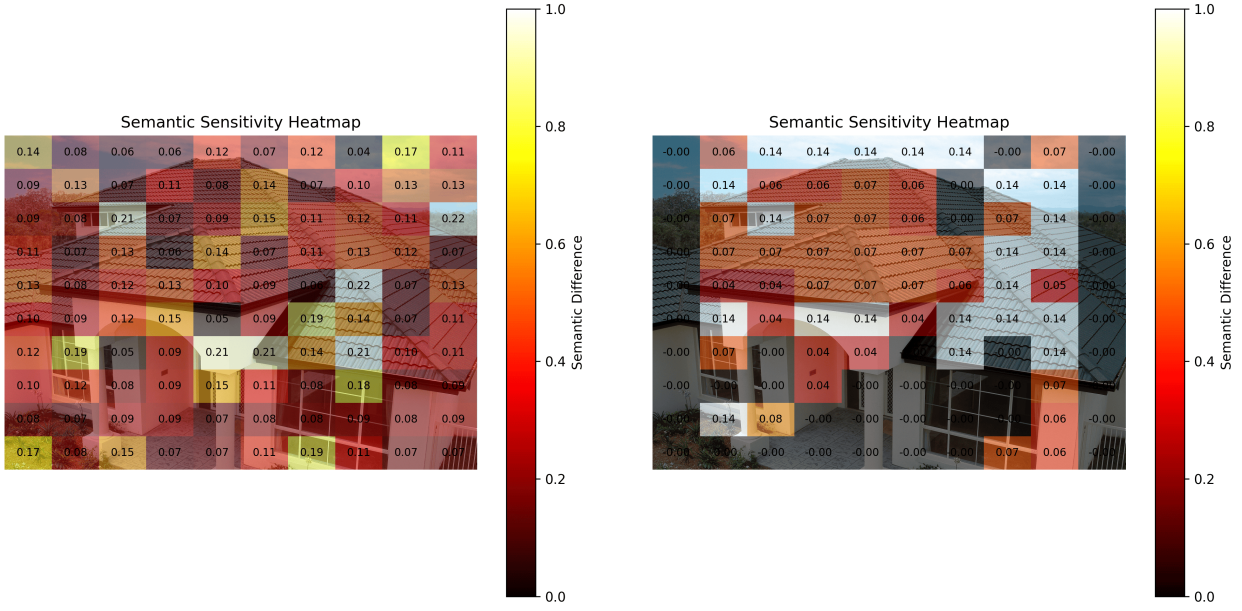


(a) GPT Heatmap



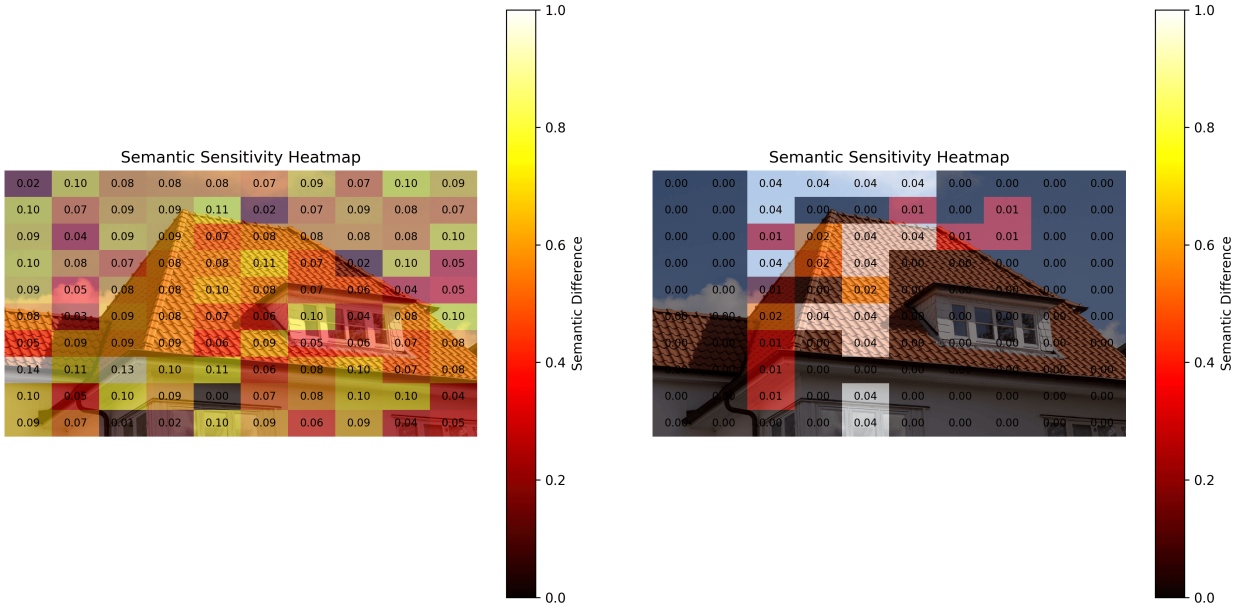
(b) LLaVA Heatmap

Figure 16. Forward Occlusion—Damaged Roof 10



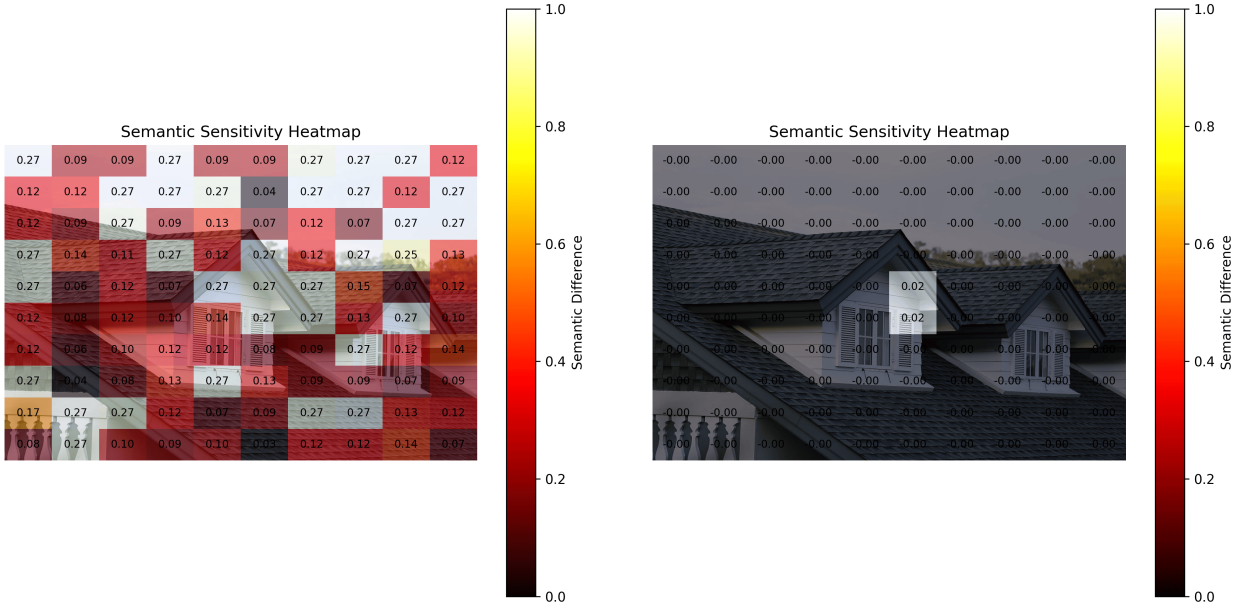
(a) GPT Heatmap **(b)** LLaVA Heatmap

Figure 17. Forward Occlusion—Undamaged Roof 1



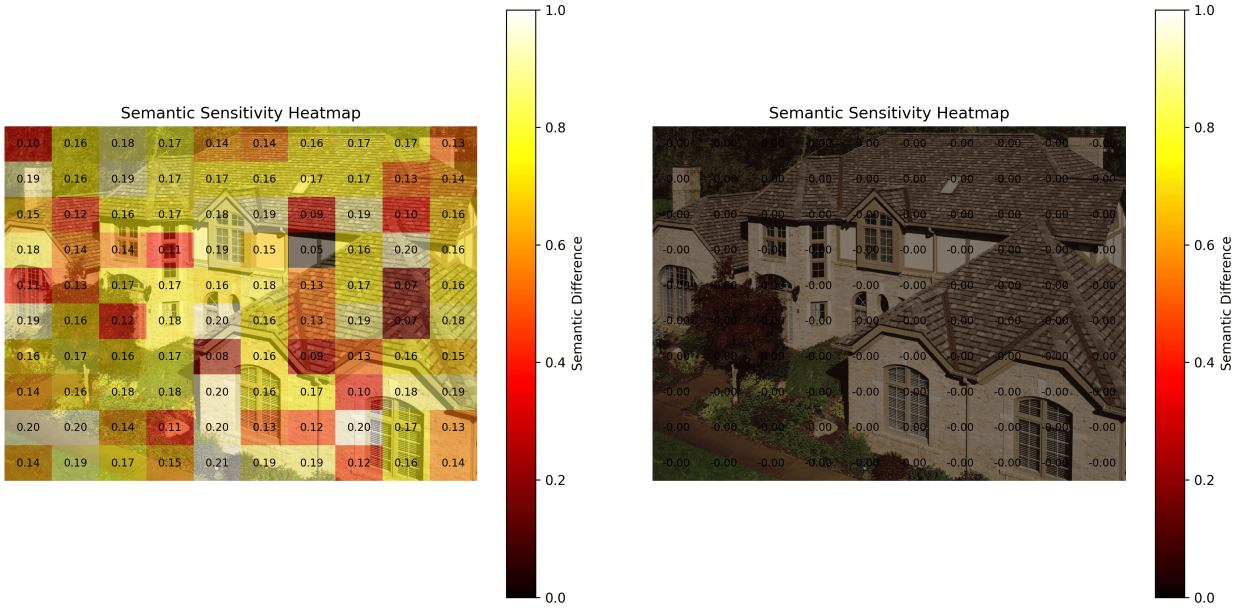
(a) GPT Heatmap **(b)** LLaVA Heatmap

Figure 18. Forward Occlusion—Undamaged Roof 2



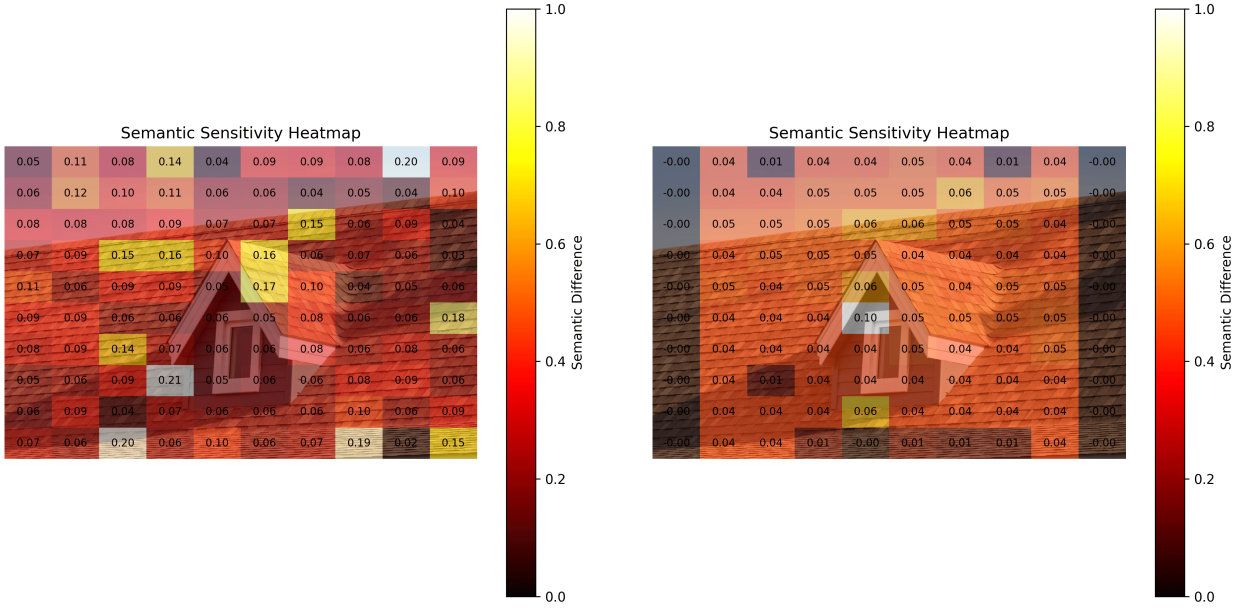
(a) GPT Heatmap **(b)** LLaVA Heatmap

Figure 19. Forward Occlusion—Undamaged Roof 3



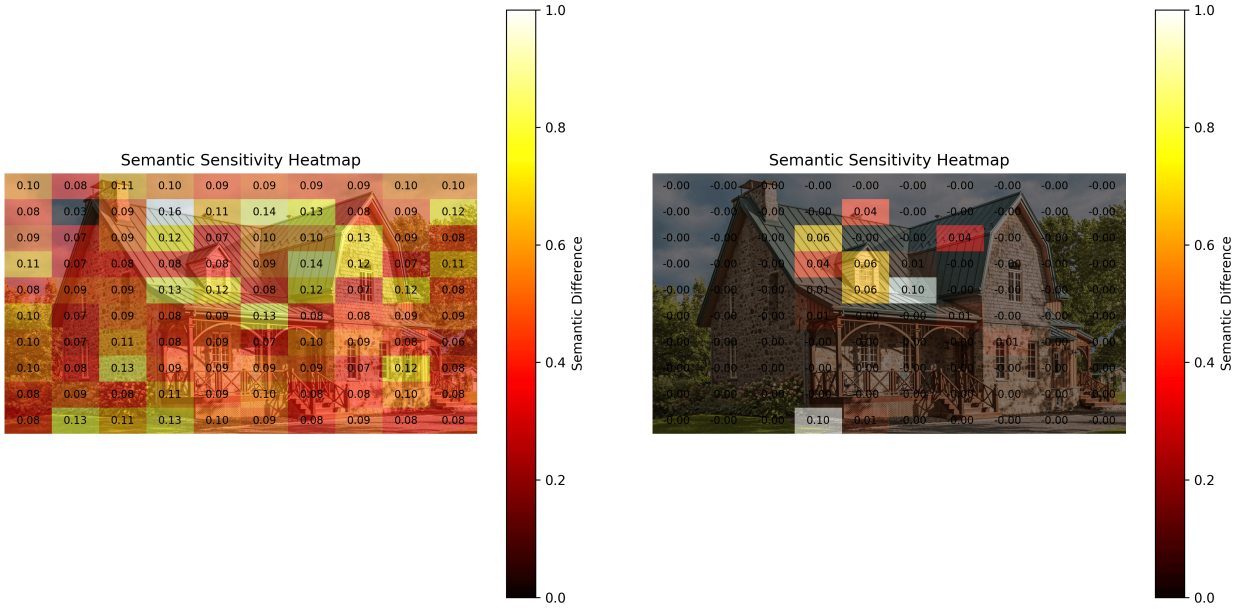
(a) GPT Heatmap **(b)** LLaVA Heatmap

Figure 20. Forward Occlusion—Undamaged Roof 4



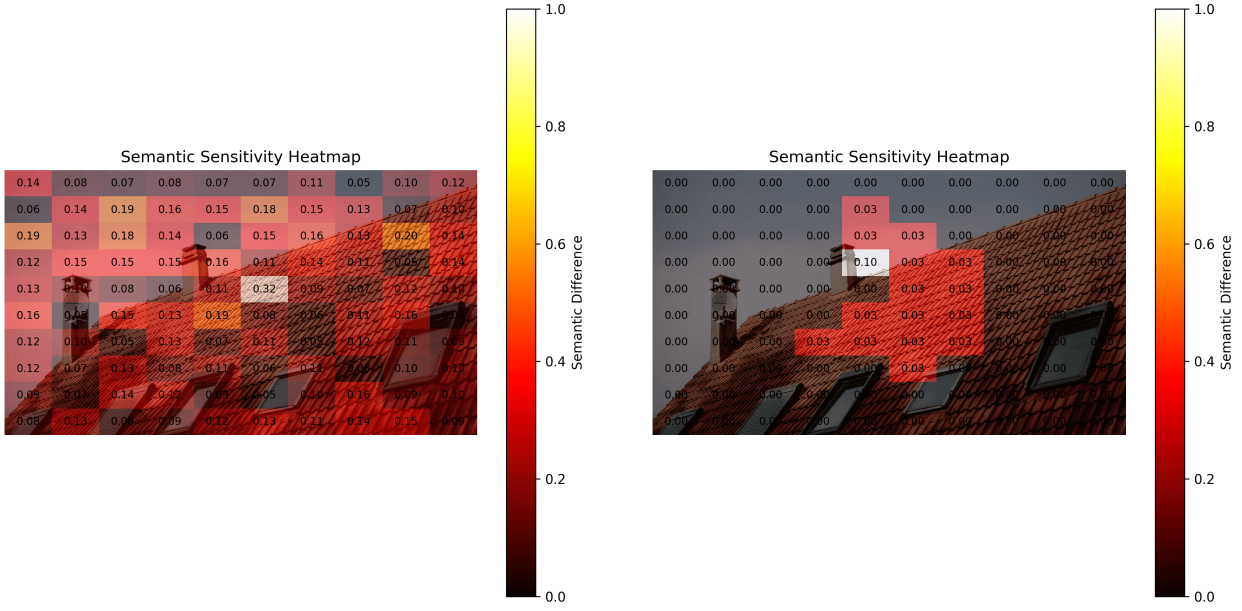
(a) GPT Heatmap **(b)** LLaVA Heatmap

Figure 21. Forward Occlusion—Undamaged Roof 5



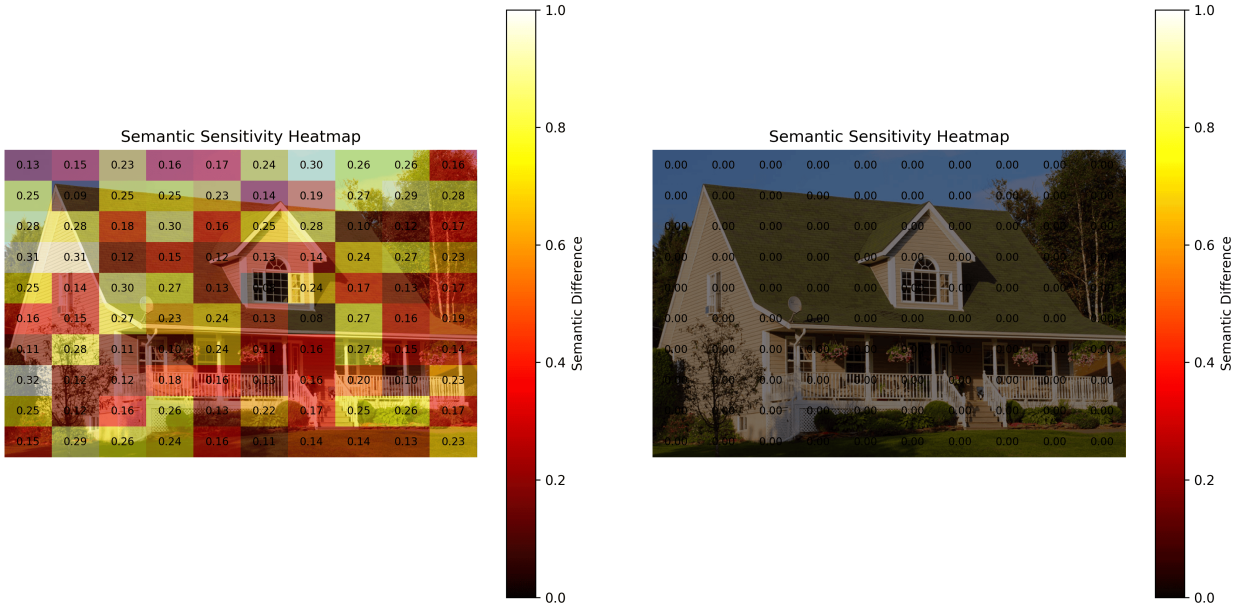
(a) GPT Heatmap **(b)** LLaVA Heatmap

Figure 22. Forward Occlusion—Undamaged Roof 6



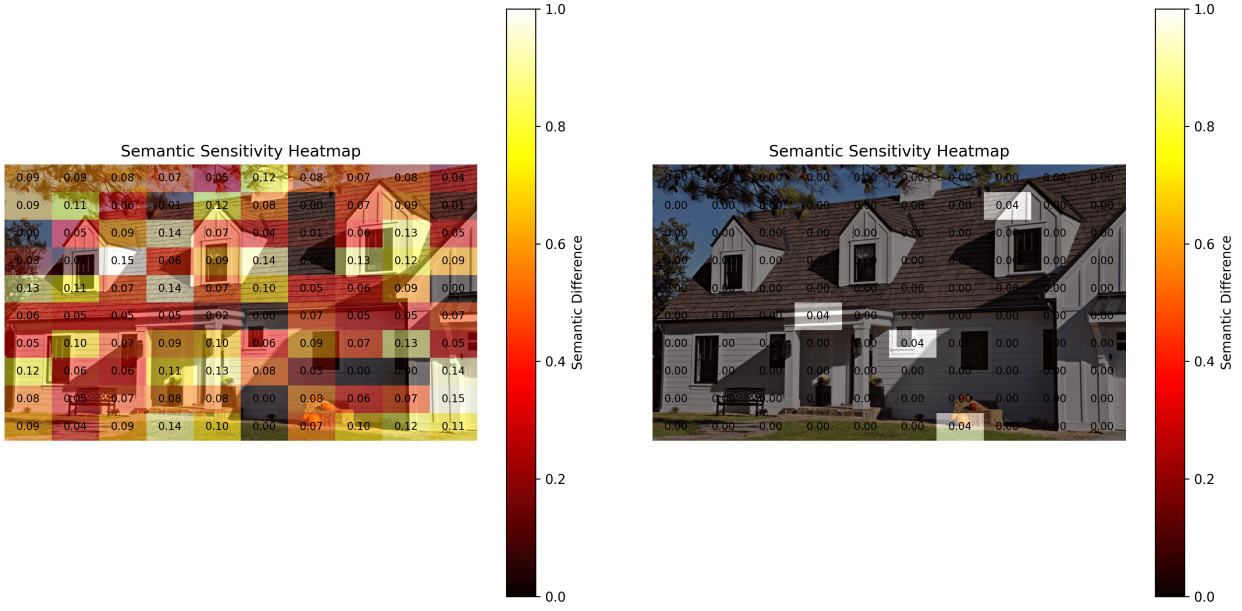
(a) GPT Heatmap **(b)** LLaVA Heatmap

Figure 23. Forward Occlusion—Undamaged Roof 7



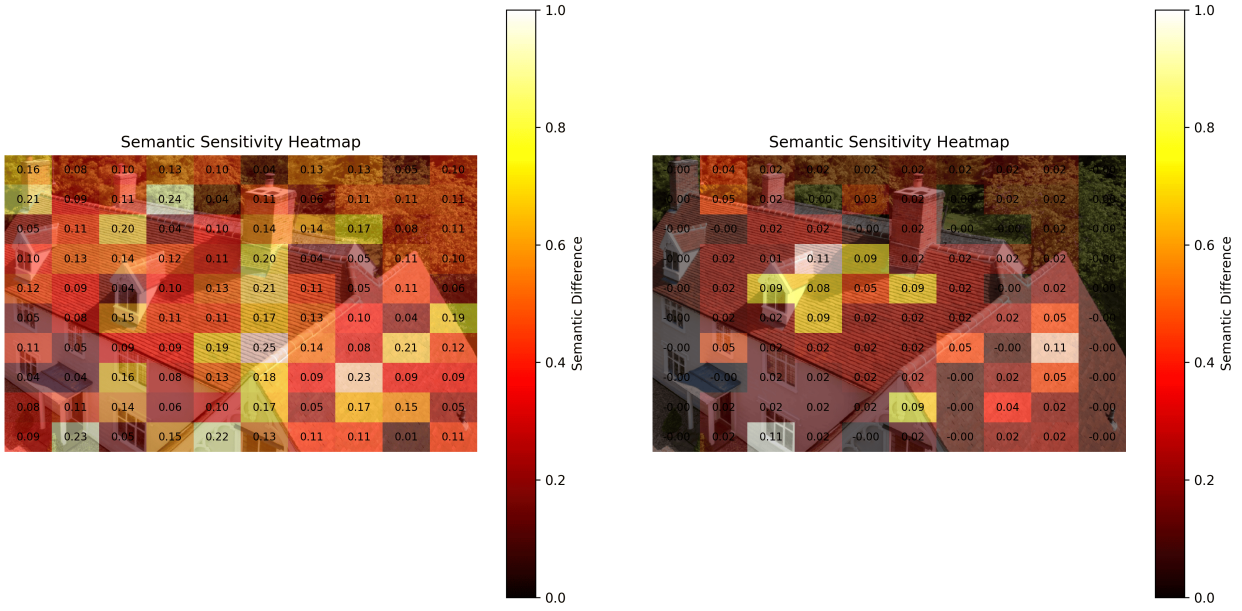
(a) GPT Heatmap **(b)** LLaVA Heatmap

Figure 24. Forward Occlusion—Undamaged Roof 8



(a) GPT Heatmap **(b)** LLaVA Heatmap

Figure 25. Forward Occlusion—Undamaged Roof 9



(a) GPT Heatmap **(b)** LLaVA Heatmap

Figure 26. Forward Occlusion—Undamaged Roof 10

B GeoJSON Generation Prompt

In this appendix, we provide the prompts used to generate the GeoJSON data in Section 3.3. First, we list the main prompt, then the retry prompt for unreasonable geometry.

```
You are a certified home energy inspection expert and data specialist building synthetic
    training data for an AI model.

You are provided with:
- Structured residential property data (JSON).
- A detailed exterior description of the home: "{exterior_description}"
- A detailed floorplan description: "{floorplan_description}"

Your tasks:
1. Generate a **GeoJSON file** for this building with:
- A plausible (longitude, latitude) location in Bethlehem, PA.
- A "FeatureCollection" containing exactly **one Feature**.
- Geometry: Polygon or MultiPolygon representing an approximate simulation-ready building
    footprint.
- The geometry should be realistic in scale for the reported square footage, number of stories,
    and building style.
- Use the floorplan description to infer approximate shape, but use the structured property data
     to control scale.
- Target approximate footprint area: {target_footprint_text}.
- The generated polygon should represent the building footprint, not the parcel or lot boundary.
- The polygon area should be within approximately 20-30% of the target footprint area when
    possible.
- Avoid large coordinate spans. For typical residential homes in Bethlehem, PA, longitude/
    latitude differences should usually be very small.
- Properties from the provided JSON:
   - "Year Built"
   - "Total Square Feet Living Area"
   - "Building Style"
   - "Exterior Wall Material"
   - "Heating Fuel Type"
   - "Heating System Type"
   - "Heat/Air Cond"
   - "Bedrooms"
   - "Full Baths"
   - "Half Baths"
   - "Basement"
   - "Number of Stories"
   - "Grade"
- Estimated performance parameters:
   - "hvac_heating_cop" (0-1)
   - "hvac_cooling_cop"
   - "wall_r_value"
   - "roof_r_value"
   - "air_change_rate" (0-1)

2. Write a short **inspection note** as if you had toured the home, focusing on energy-related
    observations: insulation, HVAC type/age, visible windows, and any inferred upgrades.
```

```
**Strict Guidelines:**
- Only base your outputs on the provided data and descriptions.
- Do not invent details not clearly supported by the inputs.
- Ensure the GeoJSON is valid and realistic.
- Coordinates should place the home plausibly in Bethlehem, PA.
- Do not generate parcel-sized rectangles.
- Do not use coordinate differences such as 0.0005 degrees unless the resulting footprint area
    is consistent with the target footprint area.
- Prefer compact residential-scale polygons.

Here is the structured property data:

{json.dumps(house_data)}

**Output Format:**
Return a raw JSON object:
{{
  "geojson": {{
    "type": "FeatureCollection",
    "features": [
      {{
        "type": "Feature",
        "geometry": {{ ... }},
        "properties": {{
          ...,
          "air_change_rate": ...,
          "hvac_heating_cop": ...,
          "hvac_cooling_cop": ...,
          "wall_r_value": ...,
          "roof_r_value": ...,
        }}
      }}
    ]
  }},
  "inspection_note": "..."
}}
No backticks or explanation.
```

```
{original_prompt}
IMPORTANT CORRECTION:
Your previous GeoJSON geometry was rejected because its footprint area was not realistic in
    scale.

Target footprint area: {last_error.get('target_area_ft2', 'unknown')} ft2
Generated footprint area: {last_error.get('generated_area_ft2', 'unknown')} ft2
Generated/target area ratio: {last_error.get('ratio', 'unknown')}

If the generated/target area ratio is greater than 1, the footprint is too large; reduce the
    coordinate span.
If the generated/target area ratio is less than 1, the footprint is too small; increase the
```

```
    coordinate span.
Adjust the footprint scale while preserving a compact residential building shape.

Regenerate the full raw JSON object, but correct the GeoJSON geometry so that:
- the footprint area is approximately consistent with the target footprint area,
- the geometry represents the building footprint, not the parcel or lot boundary,
- the coordinates remain plausible for Bethlehem, PA,
- the output remains valid raw JSON with the same top-level structure.
```